Conceptual Design of Nuclear Systems for Hydrogen Production

by

Katherine J. Hohnholt

Submitted to the Department of Nuclear Science and Engineering
in partial fulfillment of the requirements for the degree of

Bachelor of Science in Nuclear Engineering
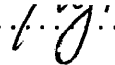
at the

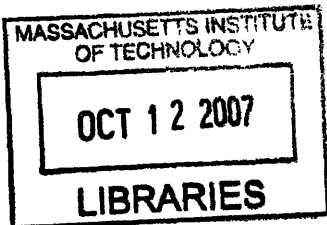MASSACHUSETTS INSTITUTE OF TECHNOLOGY

June 2006

© Katherine J. Hohnholt, MMVI. All rights reserved.

The author hereby grants to MIT permission to reproduce and
distribute publicly paper and electronic copies of this thesis document
in whole or in part.

Author ....
Department of Nuclear Science and Engineering
May 12, 2006

Certified by ....
Mujid Kazimi
Professor of Nuclear Engineering and Mechanical Engineering
Thesis Supervisor

Accepted by ....
David G. Cory
Chairman, NSE Committee for Undergraduate Students

Conceptual Design of Nuclear Systems for Hydrogen Production

by

Katherine J. Hohnholt

Abstract

Demand for hydrogen in the transportation energy sector is expected to keep growing in the coming decades; in the short term for refining heavy oils and in the long term for powering fuel cells. However, hydrogen cannot be harvested from natural sources like other fuels, it must be industrially produced. In the United States, the vast majority of hydrogen is produced today by reforming methane, a carbon-based fuel. Due to environmental and fuel source concerns, non-carbon alternatives for producing hydrogen from water are being explored using different combinations of thermal, chemical, and electrical energy. This work explores some of the non-carbon alternatives, specifically using a nuclear reactor for providing heat and electricity for high temperature steam electrolysis and a hybrid electrolysis-chemical sulfur cycle. Also addressed is the sensitivity of production and efficiency of these cycles to process conditions. For a desired hydrogen distribution pressure of 3MPa, high system pressures increase the efficiency of high temperature steam electrolysis because of the decreased post-cycle compression energy requirements. High system pressures for the hybrid sulfur cycle, however, decrease the equilibrium thermal acid decomposition necessary to the process. High temperature steam electrolysis may also be used to provide variable hydrogen production when coupled with an electricity generation system. Increased hydrogen production decreases the efficiency of the electricity production, because of the high enthalpy removed from the reactor system. Both approaches are also analyzed for their sensitivity to incomplete reactions within the process loop.

Thesis Supervisor: Mujid Kazimi
Title: Professor of Nuclear Engineering and Mechanical Engineering

Acknowledgments

Primarily, I would like to thank my advisor Professor Kazimi. He has led me patiently through this project for many years now. Also thanks to Dr. Bilge Yildiz, for getting me into this in the first place. Her patience and perseverance are incredible, and I thank her for investing so much in me.

Additionally, I would like to thank the entire nuclear engineering department. The staff, professors, and students are truly world class and I appreciate all of them tremendously. Both my education and my experience here at MIT have been outstanding and inspiring.

My deepest love and gratitude to my family: to Mom for teaching me how to dream and to Dad for keeping me grounded; to Mimi for teaching me to be meticulous and thorough and to Papa for showing me how to be calm, strong, and steady; to Daddy for his unconditional love and to Martha for telling me to fight back.

And lastly to the love of my life, Stav, who has made everything worth it.

6

Contents

List of Figures

11

List of Tables

Chapter 1

Introduction

With rising oil prices and concerns about dependence on foreign oil, America has begun to look toward alternative sources of transportation fuel. One promising alternative is hydrogen. However, one drawback of hydrogen is that it cannot be harvested from natural sources like other fuels. Hydrogen must instead be produced. Currently, the majority of hydrogen produced in the United States is produced by reforming methane, a carbon-based fuel [1][2]. However, due to environmental and fuel source concerns, non-carbon alternatives are being explored. Other methods of producing hydrogen involve using different combinations of thermal, chemical, and electrical energy to split water into hydrogen and oxygen.

This thesis will explore these non-carbon alternatives; giving background on the different methods of production, the materials concerns for hydrogen production, and a basic description of the electrolysis cells that are used to provide electrical energy to some hydrogen production cycles. The high temperature steam electrolysis and hybrid sulfur cycle will be examined in detail. To fully analyze high temperature steam electrolysis, the electrolysis unit, the heat recovery in the system, and the system compression must all be looked at in order to determine optimum component and system parameters. The hybrid sulfur cycle is a more complicated process, using the chemical energy from sulfur based compounds to assist in decomposing water

into hydrogen and oxygen. Important aspects of the design include the materials' tolerance for the chemical atmosphere, and the methods of decomposing the sulfur compounds in the cycle.

In order to avoid system problems such as blackouts, the electricity grid maintains a higher electricity supply than is demanded at any time. This leads to periods of time where there is a large amount of excess electricity generation. In these scenarios, hydrogen can be used as an energy storage device, increasing distribution efficiency by using electricity in times of low demand. The high temperature steam electrolysis process is analyzed from this viewpoint, examining the effect of varying production rates and efficiencies depending on fluctuating electricity availability.

For any realistic system design, both the speed of reactions and the relative completion of those reactions must be considered. This sensitivity is important in different ways depending upon which process is being considered.

Chapter 2

Non-Carbon Hydrogen Production Systems

2.1 Introduction

Hydrogen is currently produced worldwide for industrial applications. The United States hydrogen industry produces 9 million tons of hydrogen per year, 95% of which is produced using steam methane reforming. Most of this hydrogen production is used in chemical production, petroleum refining, metals treating, and electrical applications[1]. Hydrogen is touted as a clean, environmentally friendly alternative to current hydrocarbon fuels. However, since 95% of hydrogen is produced from hydrocarbons, alternative production techniques using non-carbon production sources have generated interest.

Hydrogen can be produced in a number of ways. Steam methane reforming mentioned above is a process that converts methane into hydrogen and carbon monoxide, as shown in Reaction (2.1)

$$CH_4 + H_2O \rightarrow CO + 3H_2 \qquad T \approx 750 - 800°C \qquad (2.1)$$
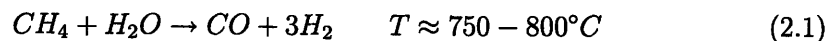
Additional hydrogen can also be extracted through this process by using the carbon monoxide in the water shift reaction, shown in Reaction (2.2).

$$CO + H_2O \rightarrow CO_2 + H_2 \qquad T \approx 350°C \qquad (2.2)$$
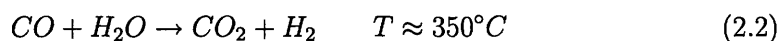
Any method using hydrocarbons, however, has the potential of releasing large amounts of global warming gases into the air, primarily carbon dioxide, but also air pollutants such as sulfur and nitrogen compounds from impurities in the hydrocarbons.

There are many alternative, non-carbon hydrogen production systems. Hydrogen can be produced by splitting water into hydrogen and oxygen. Providing the energy to do this can be done in three ways; thermally, chemically, and electrically. These energies can be used independently, but are more commonly used in conjunction with each other. Figure 2-1 shows the thermal and electrical energy requirements as a function of temperature.

Once chemical compounds are added to the process, the electric and thermal requirements can be substantially changed. By providing different pathways for completion, additional chemical components can decrease the activation energy, thus decreasing the total energy requirement for the process.

2.2 Thermal Production

Water can be split using pure thermal energy. This process is called pyrolysis and the pyrolysis temperature of water is at $\sim 4000°C$. As shown in Figure 2-1, when the temperature rises above $\sim 4000°C$, Gibbs free energy becomes less than zero and the reaction becomes spontaneous. Splitting water using pyrolysis is generally seen as unfeasible because of the extremely high temperatures required.
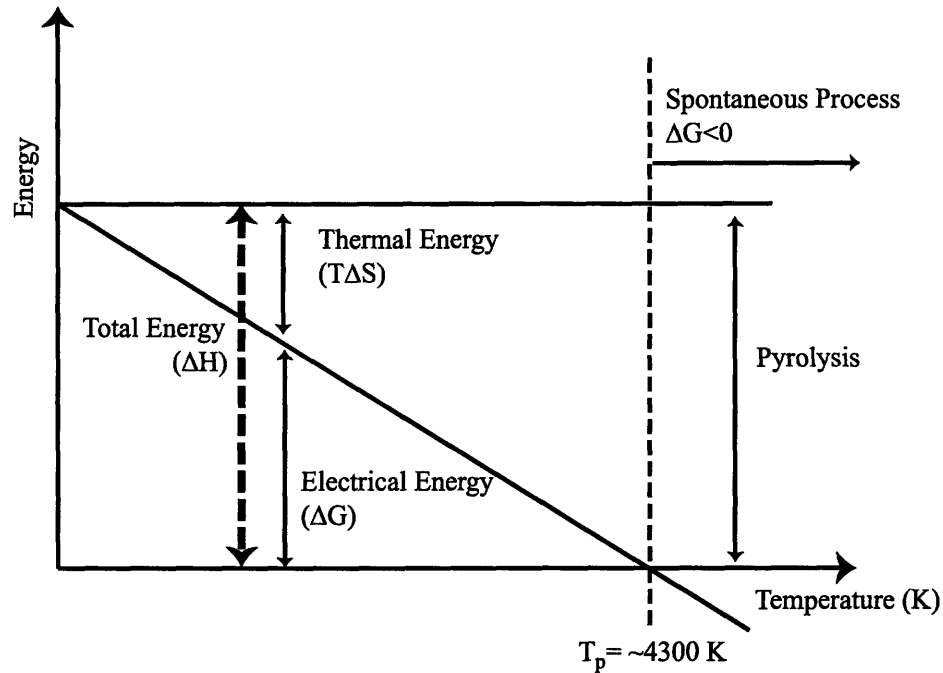
Figure 2-1: Gibbs free energy

2.3 Electrical Production

Pure electrolysis of water is the process of running a current through pure water, which provides the energy necessary to separate the water into hydrogen and oxygen. For a water electrolysis reaction at room temperature and atmospheric pressure, the theoretical minimum potential across the electrolyzer (the Nernst potential) is $-1.23V$, and the production will be proportional to the current. This is shown as Reaction (2.3) (calculated at 1 atm and 298K).

$$H_2O + e \rightarrow H_2 + \frac{1}{2}O_2 \qquad E^\circ_{cell} = -1.23V \tag{2.3}$$
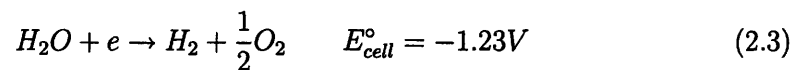
This theoretical minimum is not observable in a real cell though, as once any current is applied to the cell, gradients are created. The larger these gradients are, the more the cell can produce, however the cell will also experience larger losses. There

are also many factors within a particular cell that can change the Nernst potential in that cell. These factors, called overpotentials, include the partial pressures of the reactants and products within the cell, and the material properties of the cell. The important material properties are the exchange current density (related to the activation/kinetic losses within the electrodes), the limiting current density (related to the diffusion losses within the electrodes), and the ionic diffusion constant (related to the ionic transport losses through the electrolyte). The governing equations of these effects in the cell are given in Section 2.6. The effects of these overpotentials on the cell voltage required is shown in Figure 2-2.
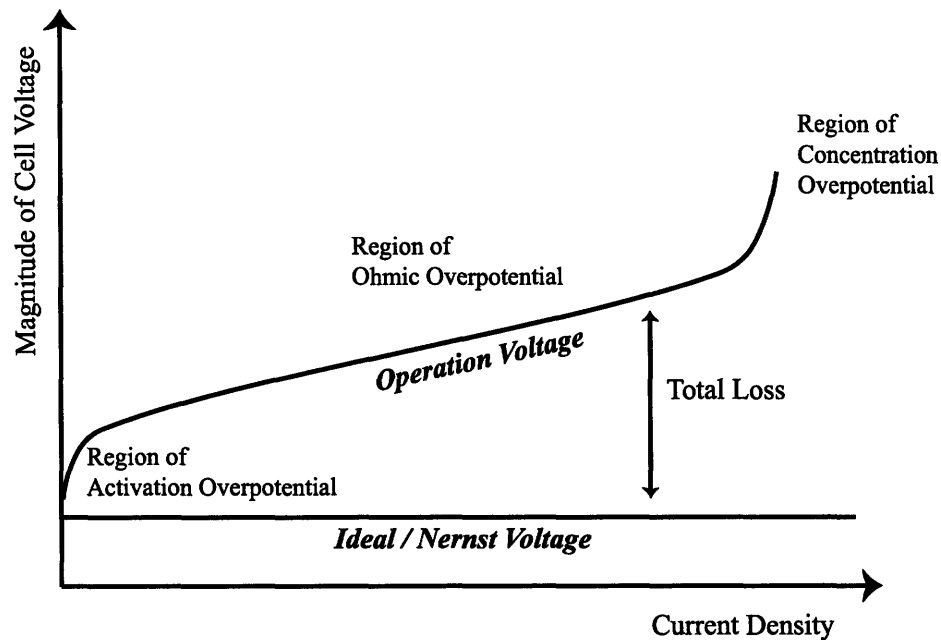
Figure 2-2: Effect of increasing current density on voltage requirement

The region of activation overpotential is the level of current through the cell where the exchange current density dominates the losses in the cell, the region of ohmic overpotential is the level of current through the cell where the ionic transport losses and electrical resistance dominate in the cell, and the region of concentration overpotential is the level of current through the cell where the limiting current density

dominates the losses in the cell. As either the magnitude of the Nernst potential (due to changes in cell conditions) or the current through the cell increases, the voltage required, and thus the total energy used for production, also increases. Maximizing cell performance by decreasing the inefficiency of water electrolysis is the subject of ongoing research, including development of new electrolysis materials that will decrease the overpotentials in the cells [3][4].

2.4 Hybrids

2.4.1 Thermo-Chemical

It may be more attractive to use a variety of energy sources instead of just one to produce hydrogen. This allows the cycle more flexibility to be optimized for production and efficiency. There have been over 180 different thermochemical water-splitting processes identified [5]. A sample of the processes that were identified as most promising, and thereby have been most investigated among these production techniques, will be described here.

The sulfur iodine process is a thermochemical cycle that uses sulfur and iodine compounds to create a chemical cycle that splits water into hydrogen and oxygen, while recycling the other species back through the system. The three reactions used in the cycle are shown below.

$$2H_2O + SO_2 + I_2 \rightarrow 2HI + H_2SO_4 \qquad\qquad 100°C \qquad (2.4)$$

$$H_2SO_4 \rightarrow SO_2 + H_2O + \frac{1}{2}O_2 \qquad\qquad 850°C \qquad (2.5)$$

$$2HI \rightarrow I_2 + H_2 \qquad\qquad 450°C \qquad (2.6)$$
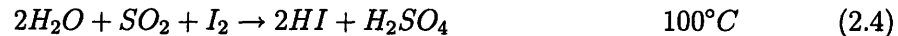
In Reaction (2.4) iodine and sulfur-dioxide are added to water to produce sulfuric acid and hydrogen iodide. The species are then separated and decomposed. Reaction

(2.5) shows the decomposition of sulfuric acid down into sulfur dioxide, water, and oxygen. Reaction (2.6) shows the decomposition of hydrogen iodide to iodine and hydrogen. Once the decomposition finishes, the oxygen and hydrogen are removed, and all other species are returned to Reaction (2.4). The sulfur iodine process has been researched extensively, and lab scale experiments have been conducted [6][7].

There are also a few variants of the Calcium-Bromine type cycles, an example is shown below (UT-3 cycle). These cycles rely on calcium, bromine, and iron to chemically separate the water.

$$Br_2 + CaO \rightarrow CaBr_2 + \frac{1}{2}O_2 \qquad\qquad 600°C \qquad (2.7)$$

$$CaBr_2 + H_2O \rightarrow CaO + 2HBr \qquad\qquad 750°C \qquad (2.8)$$

$$Fe_3O_4 + 8HBr \rightarrow Br_2 + 3FeBr_2 + 4H_2O \qquad\qquad 300°C \qquad (2.9)$$

$$3FeBr_2 + 4H_2O \rightarrow Fe_3O_4 + 6HBr + H_2 \qquad\qquad 600°C \qquad (2.10)$$
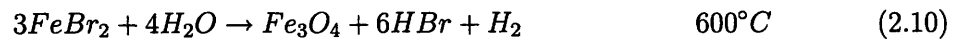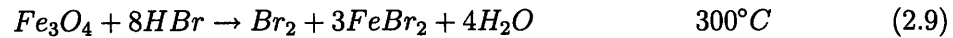
The basic process is to split water and produce oxygen in Reactions (2.7) and (2.8), regenerate bromine in Reaction (2.9), and produce hydrogen in Reaction (2.10). Ongoing research into this process is also being conducted [8].

2.4.2 Thermo-Electrical

High Temperature Steam Electrolysis (HTSE) is identical to regular electrolysis, except that the electrolytic cell is kept at a much higher temperature, around $900°C$. By running at this higher temperature, a portion of the Gibbs free energy is provided thermally, making the Nernst potential for the cell, and thus the voltage required for production, much lower. The process for HTSE is shown in Reaction (2.11) (calculated for 1 atm).

$$H_2O + e \rightarrow H_2 + \frac{1}{2}O_2 \qquad E°_{cell} = -0.933V \ at \ 900°C \qquad (2.11)$$
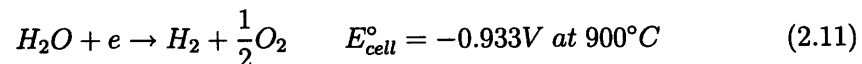
HTSE is also the subject of active research, from its potential in a solid oxide electrolytic system [9][10] to electrolyzer design [11], including system level modelling [12][13]. The specifics of HTSE will be explored more in Chapter 3.

2.4.3 Thermo-Electro-Chemical

Some cycles can even take advantage of all three energy types; thermal, electrical, and chemical. One example of this is the Hybrid Sulfur cycle. This cycle uses sulfur compounds as the chemical constants throughout the steps, and utilizes both an electrolysis step (Reaction (2.12)) and a thermal decomposition step (Reaction (2.13)). There is ongoing research on this process, including preliminary lab scale experiments [14][15][16].

$$SO_2 + 2H_2O + e \rightarrow H_2SO_4 + H_2 \qquad\qquad E^\circ_{cell} = -0.17V \qquad (2.12)$$

$$H_2SO_4 \rightarrow SO_2 + H_2O + \frac{1}{2}O_2 \qquad\qquad 850^\circ C \qquad (2.13)$$

One variant of this cycle replace Reaction (2.13) with two reactions, the first being a thermal decomposition(Reaction (2.13a)) at a much lower temperature, and the second being an electrolytic step to complete decomposition (Reaction (2.13b)). The Hybrid sulfur cycle and this variant will be discussed at length in Chapter 4.

$$SO_2 + 2H_2O + e \rightarrow H_2SO_4 + H_2 \qquad\qquad E^\circ_{cell} = -0.17V \ at \ STP \qquad (2.12)$$

$$H_2SO_4 \rightarrow SO_3 + H_2O \qquad\qquad > 450^\circ C \qquad (2.13a)$$

$$SO_3 + H_2O + e \rightarrow SO_2 + H_2O + \frac{1}{2}O_2 \qquad\qquad E^\circ_{cell} = -0.15V \ at \ 600^\circ C \qquad (2.13b)$$

There is additional research into sulfur compound separation methods using inorganic membranes [17][18].

Other thermal electrochemical hydrogen production cycles that have been re-searched are Copper-Chlorine, Copper-Sulfur, Zinc-Sulfur, and Potassium-Bismuth [19]. These cycles all use processes that take advantage of a combination of chemical, electrical, and thermal energy in unique ways.

2.5 Materials Concerns

There are significant materials concerns for each of the cycles, including high temper-ature, strength, and corrosion [20]. Materials must be tested for stability in different chemical environments, minimizing not only corrosion, but also adverse chemical in-teraction with that environment. In addition, for cycles with an electrolytic step, the choice of electrodes and electrolyte is very important not only from a stability standpoint, but also to from a performance perspective.

There is ongoing research being performed for both system and electrolysis ma-terials. In order to choose appropriate materials for the sulfur environment in the hybrid sulfur cycle, ceramic [21] and silicon carbide [22] materials are being devel-oped. Electrodes, evolving oxygen [23] and hydrogen [24] and the electrolyte within the cell [25] are all crucial to cell performance, stability, and production. There is also system level work on the potential for high temperature transfer into the cycle and its effect on materials, heat exchangers, and loop dynamics [26].

2.6 Electrolysis Cells

Basic electrochemical cells are designed to allow oxidation-reduction reactions to oc-cur, and by placing two electrodes in solution, either draw or provide a current through the cell setup.

There are many types of electrochemical cells, developed mainly for use in fuel cells. One type of electrochemical cell that has been found suitable as an electrolysis

cell is the solid oxide electrolysis cell (SOEC). An example of a SOEC electrolyzer will be shown in section 3.1.1.

Another common electrochemical cell is the proton exchange membrane (PEM) cell. This cell works by conducting protons instead of ions through it's electrolyte. Ongoing work for utilizing PEM cells in electrolysis is being conducted [27][28].

The physical principles governing electrochemical cells are primarily dependant upon the operating conditions of the cell and the material characteristics of that cell. The governing equations given below use water electrolysis to demonstrate the effect of reactants and products on the electrochemical cell operation.

The theoretical minimum voltage is calculated as a function of temperature and pressure as given in Equation (2.14). The second term gives the partial pressure dependence for V_{min} and is independent of Gibb's free energy, ΔG_o. However, the first term must be found as a function of temperature for the given reaction. This expression is the Nernst potential for the cell as a function of temperature and partial pressures of the species.

$$V_{min} = \frac{-\Delta G}{n_e F} = \frac{-\Delta G^\circ}{n_e F} - \frac{RT}{n_e F} \quad ln \left[\frac{P_{H_2} P_{O_2}^{1/2}}{P_{H_2O}} \right] \qquad (2.14)$$

The exchange current density, i_o, is related to the activation losses intrinsic to electrochemical reactions that occur within the electrodes, and is a function of the temperature and species partial pressures, as given in Equation (2.15). Experimental data showing a relation between the cell temperature and exchange current density [29] can be compared with known ranges of γ and E_{act} to produce a close fit.

$$i_o = \gamma_{electrode} \left(\frac{P_{O_2}}{P_{total}} \right)^{0.25} e^{\left(\frac{E_{act}}{RT} \right)} \qquad (2.15)$$

The exchange current density is used to determine the final current through the cell.

The binary diffusivity dominates the gas diffusion losses that occur within the

flow channels and porous electrodes. The binary diffusivity of the gases in the cell is dependant upon the gas properties, pressure, and temperature within the cell. The binary diffusivity of gas A into gas B, D_{AB}, is related to the gas properties and temperatures within the cell as given in Equation (2.16) [30].

$$D_{AB} = \frac{\varepsilon}{\tau} 1.8583 \times 10^{-7} \left(\frac{1}{M_A} + \frac{1}{M_B} \right)^{1/2} \frac{T^{3/2}}{P\sigma_{AB}^2 \Omega_{AB}} \tag{2.16}$$

The limiting current density, i_l, is related to the diffusion losses intrinsic to movement of reactants for electrochemical reactions that occur within the electrodes, and is a function of the temperature and the porous diffusivity of the reactants and products. The limiting current density is related to the diffusivity, reactant concentrations, and temperatures within the cell. The limiting current is defined in Equation (2.17).

$$i_l = \frac{nFDC_{reac,bulk}}{\delta_{electrode}} \tag{2.17}$$

All of these components come together to describe the losses (called the overpotentials) in the cell. As the applied voltage within the cell increases, the overpotentials in the cell increase due to the increasing current through the cell as shown in Equation (2.18).

$$V_{applied} = V_{min} - \eta_{activation} - \eta_{diffusion} - \eta_{ohmic} \cdots \tag{2.18}$$

This means that increasing production in the cell increases the losses. The optimum level of compromise between maximum production and maximum efficiency must be decided within each system. More detail about how the current is calculated and the affects on hydrogen production is provided in Section 6.2.3.

Chapter 3

High Temperature Steam Electrolysis

3.1 Electrolysis System

3.1.1 Electrolysis Unit

Solid Oxide Electrolysis Cell

The electrolysis unit for HTSE is generally modeled using a solid oxide electrolysis cell (SOEC). A SOEC cell is composed of an oxide ion-conducting electrolyte surrounded by porous electrodes. An example of the cell configuration is shown in Figure 3-1.

The figure shows the two independent flow paths through the cell, the oxygen outlet channel (usually containing a sweep gas), and the water inlet and hydrogen production channel. The cathode provides electrons to drive the decomposition of water into hydrogen and oxygen ions. The ions are then allowed to move through the electrolyte, while the hydrogen is pushed out of the cell. Once the oxygen ions move through the electrolyte, oxygen begins to evolve on the anode, giving off extra electrons that are driven back through the cell toward the cathode by the voltage across the cell.
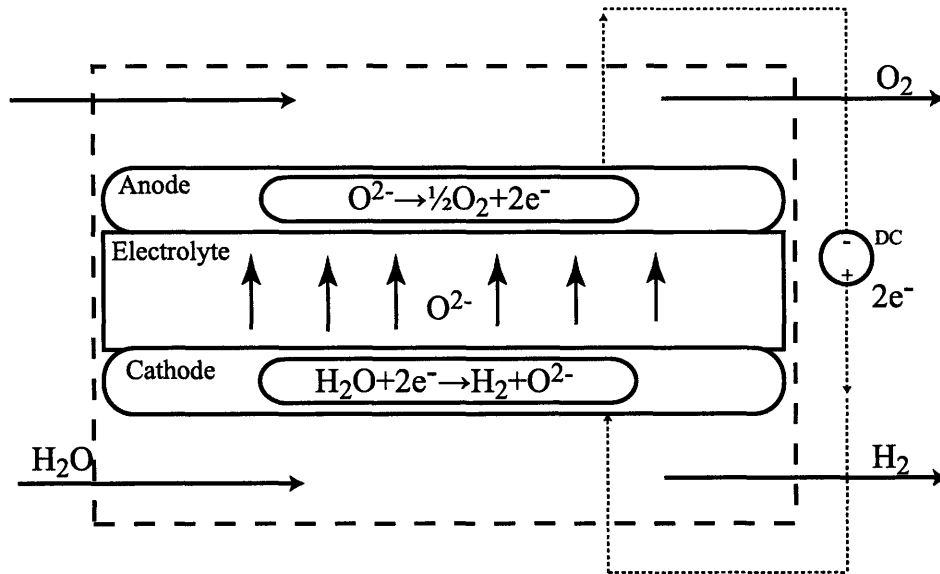
Figure 3-1: Electrolysis cell for water decomposition

3.1.2 Heat Recovery

Direct Feed

The simplest way to provide the necessary thermal energy for the electrolysis loop is to provide it directly from a single heat exchanger, with the reactor as the heat source, as shown in Figure 3-2. This system is simple, providing all the necessary increase in temperature from the reactor.

The principle disadvantage of this setup, however, is that this would require the hot loop temperature to be greater than the temperature desired in the electrolysis loop. Since the electrolysis loop is most efficient at very high temperatures, this system would only be feasible with a very high temperature thermal energy source. In addition, a tremendous amount of energy would be lost in the exiting gas streams (hydrogen and oxygen), due to their high temperature.
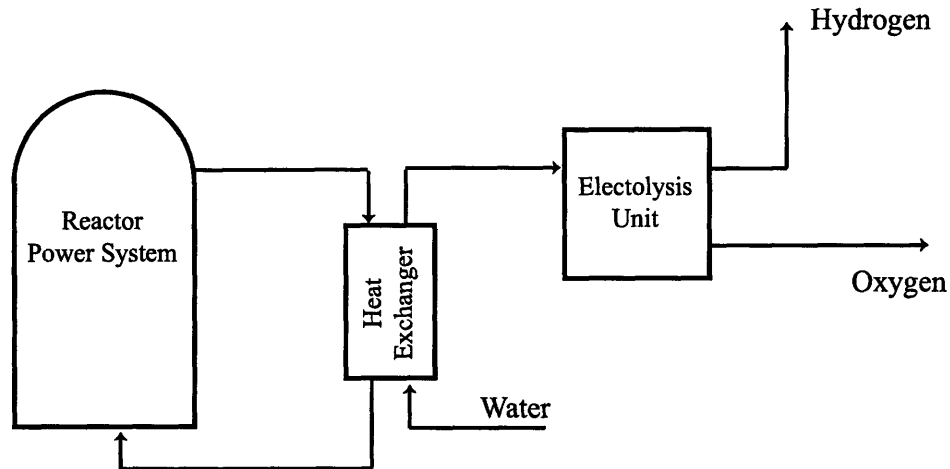
Figure 3-2: Direct input of thermal energy to electrolysis system

Dual Recuperators

By adding recuperating heat exchangers, we can tap into the thermal energy of the exiting hydrogen and oxygen streams, and avoid having to supply some heat from the reactor. An example of such a system is shown in Figure 3-3.

Both gas streams can provide high temperature thermal energy to heat the incoming steam up to a much higher temperature prior to entering the electrolysis unit. However, because of non-ideal heat transfer, both from heat losses in the heat exchanger, and energy losses at flow restrictions, the incoming steam will not be completely raised to the temperature necessary. In order to complete the last heating stage, a final electrical heater is used, as shown also shown in Figure 3-3.

Another important consideration is the amount of thermal energy that the gas streams possess. Since neither hydrogen nor oxygen will undergo a phase change in the range of temperatures of interest, the gas streams do not have enough enthalpy to overcome the heat of vaporization of water. Therefore the reactor must provide at least enough thermal energy to preheat the water through its phase change, to a quality of 1, i.e. to saturated steam conditions.
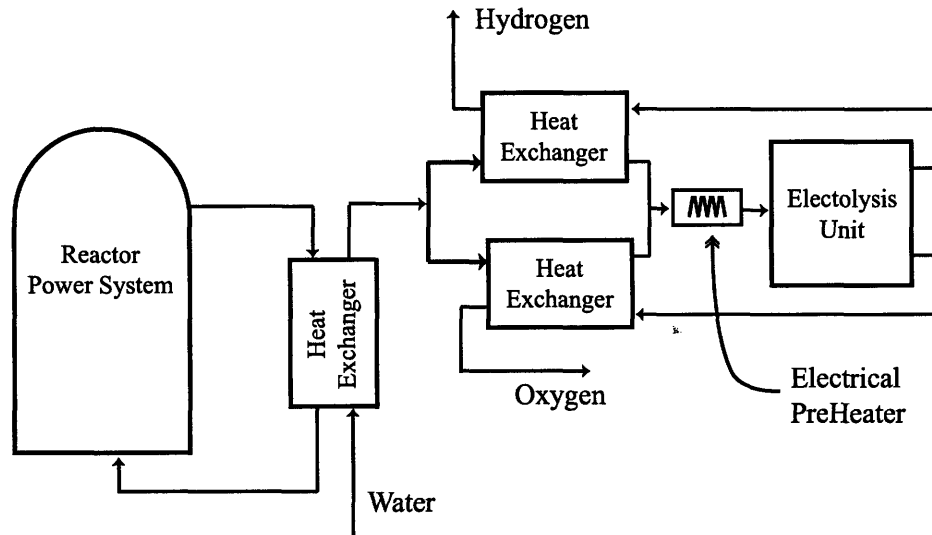
Figure 3-3: Diagram of electrolysis system with primary heat recuperation

Preheaters

Even after using the recuperators to heat the steam, there is still thermal energy available in the gas streams. The streams temperatures are now too low to contribute their thermal energy to heating the steam further, but they can serve to preheat the water before it enters the main boiler. By adding two preheaters the gas streams can be used to heat the incoming water.

Additional Recuperators

By adding additional recuperating heat exchangers, even more thermal energy can be recuperated, leading to increased efficiencies. However, with every heat exchanger added, there are diminishing returns on the increment in efficiency, as well as increasing effects on the capital costs of the system.

3.1.3 Compressors

There are many ways to distribute hydrogen, the most common forms are as a liqui-
fied gas or a compressed gas. Because of the large energy requirements of liquification,
the effects of compression on the system were examined. Existing hydrogen pipelines
compress to $\sim 7MPa$ for distribution. The production facility must compress hy-
drogen to the distribution pressure in order to send it through these distribution
networks. Two ways of compressing this hydrogen are to compress the water before
it enters the electrolysis system (pre-compression), or to compress the hydrogen once
it has been separated (post-compression).

Pre-Compression

Compressing a liquid, such as water, is much less energy intensive then compressing
a gas, such as hydrogen. Therefore precompressing the water before it enters the
electrolysis system has certain energy advantages. Compressing water from 1 atm to
7 MPa requires a pumping power of approximately 7.5 kilojoules per kg water, or
approximately 0.8 kilojoules per kg hydrogen. In addition to the energy advantage,
increased pressure in the electrolysis system will also serve to decrease the volume of
the components (pipes, heat exchangers, electrolysis cell, etc.) for the same flow rate.

Post-Compression

The disadvantage to the pre-compression idea, however, is that the pressure in the
system will change the operating conditions, energy requirements, and material re-
quirements in the electrolysis system. These effects are described in section 3.2.1.
Compressing the hydrogen after it exits the electrolysis cell is a viable alternative,
but requires a larger compression energy of approximately 48 kilojoules per kg hy-
drogen for compression from 1 atm to 7 MPa.

3.2   Component Optimization

3.2.1   Pressure Effects on Component Design

By increasing the pressure within the system, there are important effects for the components operation within the system. First of all, the electrolysis cell properties will change because the Gibbs free energy of the reaction has increased due to the higher system pressure. Therefore the magnitude of the voltage required in the electrolysis cell increases. This raises the total energy required for the electrolysis process, decreasing the system's efficiency.

This efficiency loss can be offset, however due to the positive relation between pressure and efficiency in the heat exchangers and compressor. Within the heat exchangers the higher pressure increases the heat capacity of the fluids being fed through the exchangers, meaning that the fluids have more energy per mol to contribute. Additionally, since the fluids are also compressed, there are more mols per volume, and thus more energy per volume available for exchange.

The system pressure is very important for system compression, because where the compression occurs changes the type of compression that is needed. If the total system pressure is low, then the product gas must be compressed after exit before it is fed into the distribution system. Gas compression is very energy intensive, requiring a qualified compressor. However, if the system is run at a higher pressure, the water must be pumped into the system. Pumping this liquid is much less energy intensive, as discussed in the section on compression, requiring only a simple water pump.

3.3   System Optimization

3.3.1   Interface with Reactor

The proposed system set up receives all of its thermal and electrical energy requirement from some sort of reactor. For that thermal requirement, it is important to

consider where the thermal energy will be drawn from the power cycle. There are two main ways to divert this thermal energy, both illustrated in Figure 3.3.1. Drawing off any thermal energy will necessarily decrease the efficiency of the reactor power system, but its effect can be minimized by placing the heat exchanger after the power cycle, prior to the coolants entrance back to the reactor as illustrated in Figure 3-4(a). This way the maximum temperature will still be at the entrance to the power cycle turbines, delivering maximum efficiency through them, however this is only feasible it the temperature is still high enough for the thermal requirements of the HTSE system. This fact makes HTSE most feasible with a higher temperature reactor, where the temperature requirements of an additional electrolysis system would not be so close to the operating temperatures of the reactor.

(a) High efficiency configuration   (b) Split flow configuration
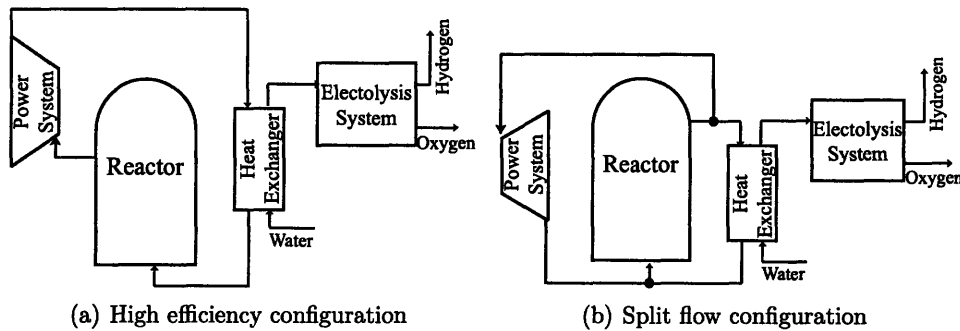
Maximizing the efficiency of the power cycle is important because the efficiency of HTSE is almost directly dependant upon the electrical efficiency of the reactor. This is because hydrogen production is proportional to the current provided in the electrolysis cell. Therefore an optimum reactor for this application would have very high base efficiency. The thermal energy drawn off of the reactor system will decrease this efficiency, but with a high enough initial efficiency, this drop should be acceptable.

The reactor coolant temperatures have to be above the boiling temperature of the water in the electrolysis system. This means that is the HTSE is running at low pressure, even water cooled reactors can supply sufficient heat. However for these lower temperatures it is necessary to send the maximum temperature into the

HTSE system. This split flow type system is illustrated in Figure 3-4(b). It is very important to note though that this process is directly taking away thermal power from the reactor system, that would have instead gone to power conversion. Another benefit of the split flow system is the ability to regulate flow rates very easily. This ability is advantageous if adjustable production rates are desired (discussed in Chapter 5).

3.3.2 Pressure Effects on System Design and Efficiency

As discussed above, there are important energy requirement effects for the choice of system pressure. Increasing pressure increases the energy required in the electrolysis cell, but decreases the energy required for pumping and makes the heat exchangers more efficient. There is also an overall effect on system design to consider when choosing the optimum operating pressure. With increased pressure, the volume of all of the components of the system can be decreased while delivering the same production rate. This results in a significant change in the capital costs of each of these components. Smaller designs equate almost directly to lower capital costs.

Normally efficiency is calculated by dividing the resulting energy (ΔG_{H_2}, the low heating value (LHV) for hydrogen is used in this work) by the energy input ($\Delta G_{reactor}$, the total energy produced by the reactor). This can also be defined in terms of the thermal and electrical energy requirements ($\Delta G_{thermal}$ and $\Delta G_{electrical}$) along with the efficiency of producing the electrical requirement ($\eta_{powercycle}$). These relations are shown in Equation (3.1). The thermal and electrical requirements are based on Gibb's free energy of the reaction (illustrated in Figure 2-1) and the efficiency of the power cycle was calculated using the modeling of Dr. Dostal [31].

$$\eta_{H_2production} = \frac{\Delta G_{H_2,LHV}}{\Delta G_{reactor}} = \frac{\Delta G_{H_2,LHV}}{\Delta G_{thermal} + \frac{\Delta G_{electrical}}{\eta_{powercycle}}} \tag{3.1}$$

By including the effects of compression costs and electrical losses, the practical

usefulness of the efficiency calculation is increased. This can be done by calculating the work required by any pumping (W_P) or compression (W_C) in the system and incorporating it into the efficiency calculation (Equation (3.2)).

$$\eta_{H_2production} = \frac{\Delta G_{H_2,LHV}}{\Delta G_{thermal} + \frac{\Delta G_{electrical}+W_P+W_C}{\eta_{powercycle}}} \tag{3.2}$$

The compression and pumping work can be calculated as a function of the compound properties, shown in Equation (3.5). Compressor (η_C) and pump (η_P) efficiencies used in this work were both 85%.

$$W_P = \frac{W_{P,ideal}}{\eta_P} = \frac{\dot{m}_{H_2O}\Delta h}{\eta_P} \tag{3.3}$$

$$W_C = \frac{W_{C,ideal}}{\eta_C} = \frac{\dot{m}_{H_2}\Delta h}{\eta_C} \tag{3.4}$$

$$= \frac{1}{\eta_C}\dot{m}_{H_2}RT\left(\frac{k}{k-1}\right)\left(\left(\frac{P_{H_2,out}}{P_{H_2,in}}\right)^{k-1/k} - 1\right) \tag{3.5}$$

The complete description of the mathematical method used to determine this efficiency has also been described in Yildiz [32], and the calculations are given in Appendix C. The same general correlation between electrical efficiency and production efficiency illustrated in Figure 3-4 holds for total efficiency, as the compression costs are the largest losses in the system, and the compressor is assumed to use electrical power from the plant. Figure 3-4 shows the effect of varying system pressures on the total efficiency and total hydrogen production at varying temperatures. The figure also assumes that the hydrogen is being compressed to a distribution pressure of 3MPa.

Due to the compression costs associated with the total efficiency, as the process pressure approaches the distribution pressure, efficiency is increased. However, higher system pressures also decrease the hydrogen production potential of the system because of increasing energy requirements for electrolysis. Another factor that has to
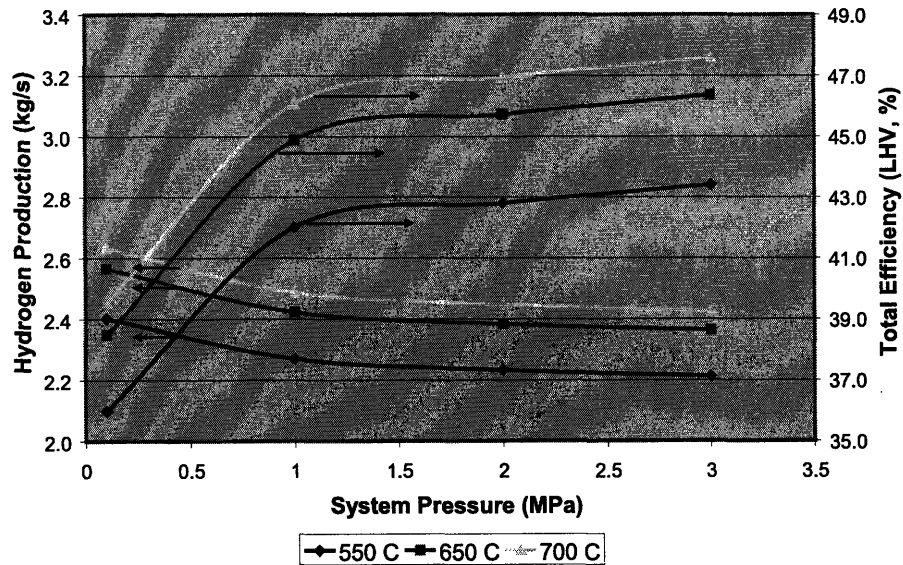
Figure 3-4: Total hydrogen production efficiency and hydrogen production at varying system pressures

be considered is the capital cost involved with plant production. As the pressure is increased, the size of system components will be decreased, however, the strength of those components will also have to increase. Given all of these considerations, the operating condition of pressure is very important, but depends greatly on the relative value of efficiency versus capital cost of the system.

3.4   Model Corrections

The model that was used to calculate the efficiency and production of the system is described fully by Yildiz [32]. The power source for these calculations was further based upon the doctoral work of Dr. Dostal [31]. Dr. Dostal modeled a supercritical CO_2 reactor cycle. His model calculated, among other things, the efficiency of this system. An additional heat exchanger was added to the model so that the enthalpy

removed for the hydrogen production cycle could be included in the calculations. The efficiency reported as net efficiency in Dr. Dostal's model was used as the total net electrical production efficiency in the hydrogen production calculations. Dr. Dostal's reported net efficiency, however, did not include certain losses in the entire system, such as pipe losses, because the efficiencies were used as if they were a total net efficiency. The error from these assumptions propagates throughout the hydrogen production calculations. It has been determined that by including the additional losses, the total net efficiency is actually between 2% to 4% less than the efficiency reported. This was determined in a model, however, that does not include the additional heat exchanger to model the enthalpy transferred into the hydrogen production system that necessarily lowers the electrical efficiency of the reactor system. Because the model has not been fully developed, the actual effect cannot yet be determined. In order to predict the sensitivity of the system to the efficiency change, the efficiency for hydrogen production has been recalculated. The efficiency was calculated for the different pressures and overpotentials previously used, changing only the net electrical efficiency used by 2% and the results are given in Table 3.1.

Pressure (MPa)	Efficiencies			Difference
	Orig Electrical	Orig H_2	Recalculated H_2	
0.1	42.7	36.3	34.7	1.6
1	42.8	41.7	39.9	1.8
2	42.8	42.4	40.6	1.8
3	42.9	42.9	41.1	1.8

Table 3.1: Sensitivity of hydrogen production efficiency to changes in net electrical efficiency

The table shows that overall efficiency increases with increasing pressure. This is because of the high energy demand from post-compression of hydrogen gas, discussed in Section 3.1.3. However, the higher pressures are more sensitive to a change in the net electrical efficiency. This is because at higher temperatures the voltage required through the electrolysis cell is higher. Combining this with lower compression energy requirements, the dominant energy demand in the system is the electrolysis cell, and

the hydrogen efficiency becomes almost directly correlated with the net electrical efficiency. Given this, we can safely assume that any decrease in net electrical efficiency will be closely followed by an equivalent decrease in hydrogen production efficiency.

Chapter 4

Hybrid Sulfur Cycle

4.1 Process Design

4.1.1 Basic Design

The Hybrid Sulfur Cycle is an alternative cycle that uses the sulfur compounds as transferring agents to produce hydrogen. Like all thermochemical cycles, the only chemical introduced into the system is water and the only substances extracted out are hydrogen and oxygen. This means that ideally the entirety of the sulfur within the system is recycled completely. The Hybrid Sulfur Cycle, illustrated in Figure 4-1, incorporates an electrolysis cell with this chemical process.

In its most basic form, the cycle has one electrolyzer that drives the production of hydrogen, used in Reaction (4.1).

$$SO_2 + 2H_2O + e \rightarrow H_2SO_4 + H_2 \qquad E^\circ_{cell} = -0.17V \qquad (4.1)$$

$$H_2SO_4 \rightarrow SO_2 + H_2O + \frac{1}{2}O_2 \qquad\qquad 850^\circ C \qquad (4.2)$$
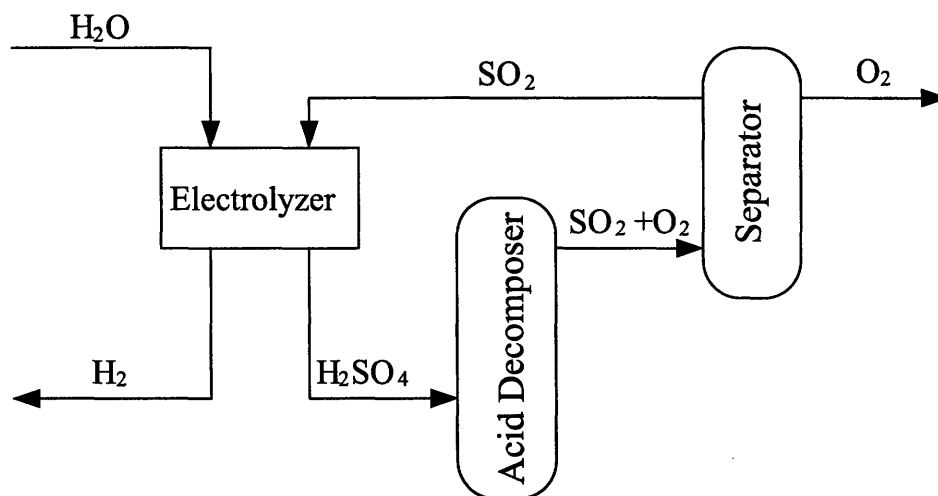
Figure 4-1: Conceptual design of hybrid sulfur cycle

After the electrolysis step, the resulting hydrogen is collected, and the sulfuric acid is recycled into the system. In order to complete Reaction (4.2), thermal energy from the reactor must be added to the acid decomposer, as shown in Figure 4-1. Once the sulfuric acid is decomposed, sulfur dioxide and oxygen exit the acid decomposer and are sent to a separator. The mixture is cooled so that the oxygen is still in gaseous form, and can be vented, and the sulfur dioxide has cooled into liquid phase, and can be separated and sent back into the electrolysis unit. Figure 4-1 shows the process diagram for a simplified version of this system.

The various chemical compounds can be separated because of the difference in their boiling temperatures, illustrated in Figure 4-2. In order to separate chemical compounds, the mixture is cooled to a point where one compound condenses and the resulting liquid can be diverted from the mixture. This process is repeated until only an aqueous solution of sulfur dioxide can be sent back to the primary electrolyzer.
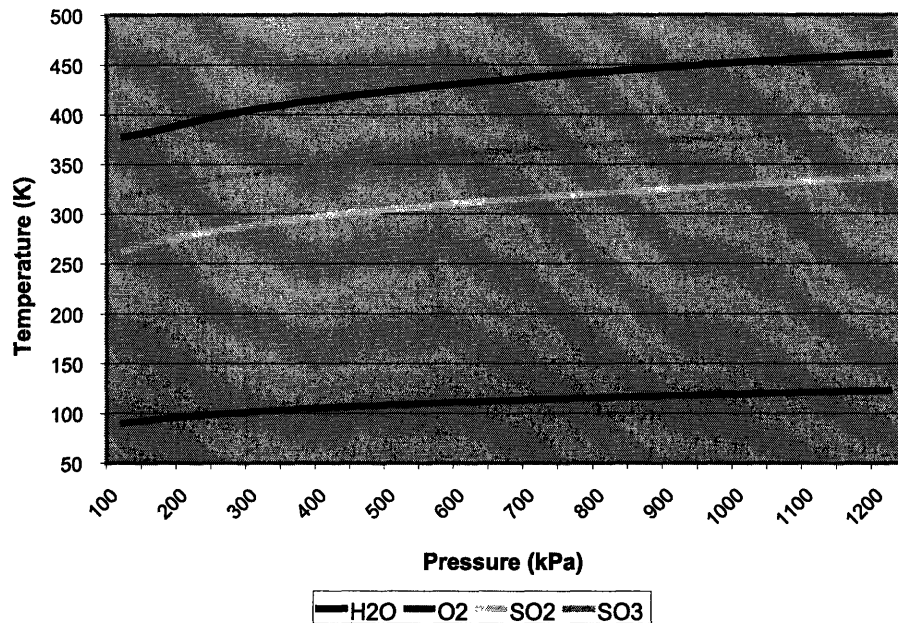
Figure 4-2: Boiling temperatures of chemical compounds in Hybrid Sulfur Cycle

4.1.2 Additional Electrolysis Design

In order to overcome the extremely high temperature requirements of the acid de-
composer, it has been proposed that a second electrolysis unit be added to assist in
the decomposition of the sulfuric acid, shown here as Reaction (4.2b).

$$SO_2 + 2H_2O + e \rightarrow H_2SO_4 + H_2 \qquad\qquad E^\circ_{cell} = -0.17V \qquad (4.1)$$

$$H_2SO_4 \rightarrow SO_3 + H_2O \qquad\qquad > 450^\circ C \qquad (4.2a)$$

$$SO_3 + H_2O + e \rightarrow SO_2 + H_2O + \frac{1}{2}O_2 \qquad E^\circ_{cell} = -0.15V \ at \ 600^\circ C \qquad (4.2b)$$
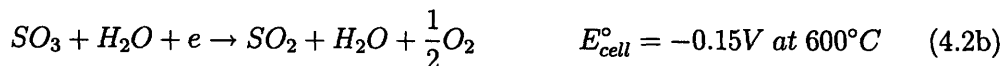
As a consequence of this change, the first part of the decomposition (Reaction
(4.2a)) can proceed at a much lower temperature, decomposing the sulfuric acid to
sulfur trioxide. The high temperature requirement in the process is for the decompo-
sition of this sulfur trioxide. By adding the electrolysis unit, the maximum required

temperature can be reduced to around 500 to 600°C, making the materials require-
ments of the process much more feasible to provide. The electrolyzer also serves to
separate the sulfur dioxide and oxygen streams. Figure 4-3 shows the process design
for a simplified version of the system.
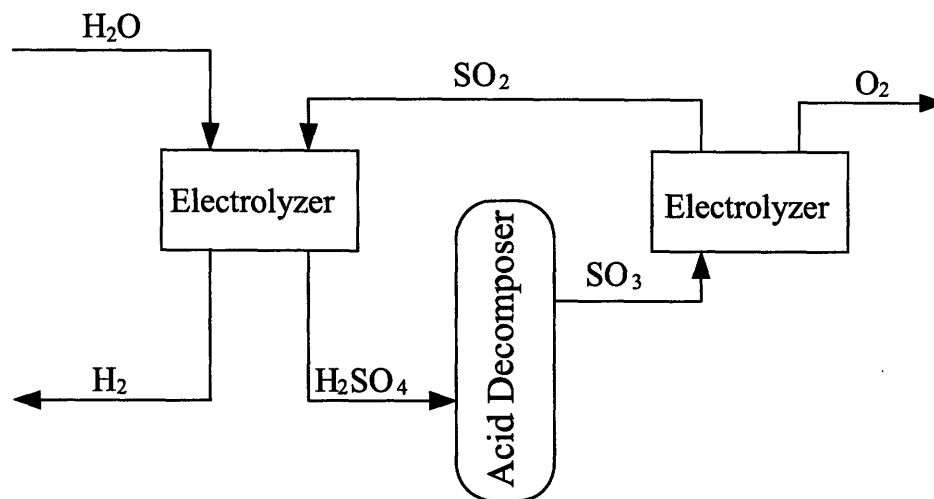
Figure 4-3: Conceptual design of hybrid sulfur cycle with dual electrolyzers

4.2   Component Design

4.2.1   Primary Electrolyzer

The primary electrolyzer used in the hybrid sulfur cycle is designed to evolve hydrogen
as product and sulfuric acid for further use in the system. The basic set up is shown
in Figure 4-4.

The figure shows the flow paths in the cell. The flow path, cathode, and electrolyte
work exactly the same as a basic water electrolysis cell. The difference in this cell is
the chemical environment that the anode is exposed to. In the anode flow path, the
oxygen combines with sulfur dioxide to produce sulfur trioxide, then further combining
with water to produce the final product of sulfuric acid. As in a water electrolysis
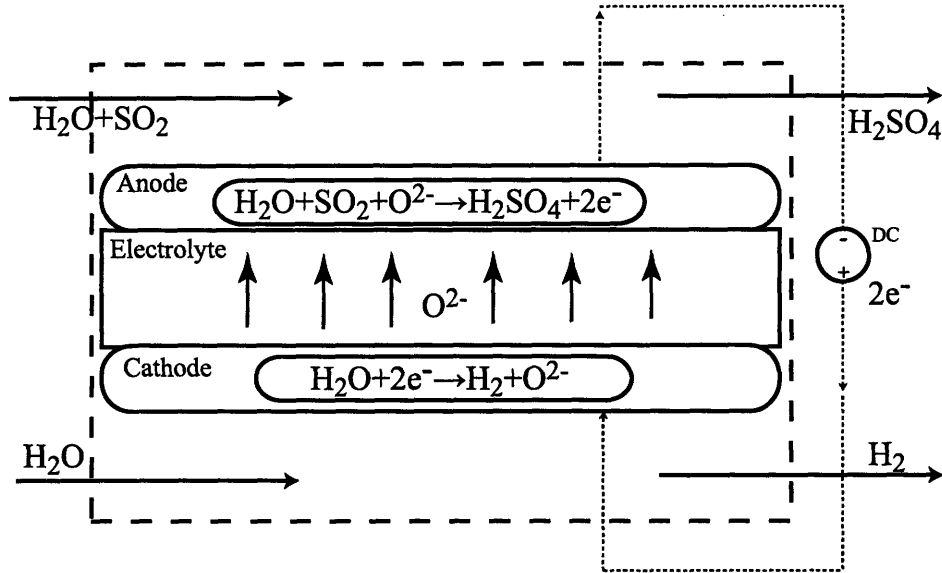
Figure 4-4: Primary electrolysis cell for hybrid sulfur cycle

cell, the excess electrons from the anode are driven by the voltage across the cell to the cathode to promote the water decomposition there.

4.2.2 Sulfur Trioxide Secondary Electrolyzer

The secondary electrolysis unit has the advantage of being similar to a water electrolysis cell. By passing oxygen ions through the electrolyte, and evolving oxygen on the anode, the electrolyte and the anode are completely analogous to those used in a water electrolysis cell. Figure 4-5 shows the basic design of the decomposition electrolysis cell.

While research and experience with the anode can be transferred from water electrolysis research, the cathode for this system is very different. The decomposition of sulfur trioxide presents several unique challenges, including choosing a suitable electrode material that will be able to withstand the sulfur environment under desirable conditions, while maintaining a high decomposition efficiency. The electrolyte must also be tested to determine its ability to withstand the sulfur environment.
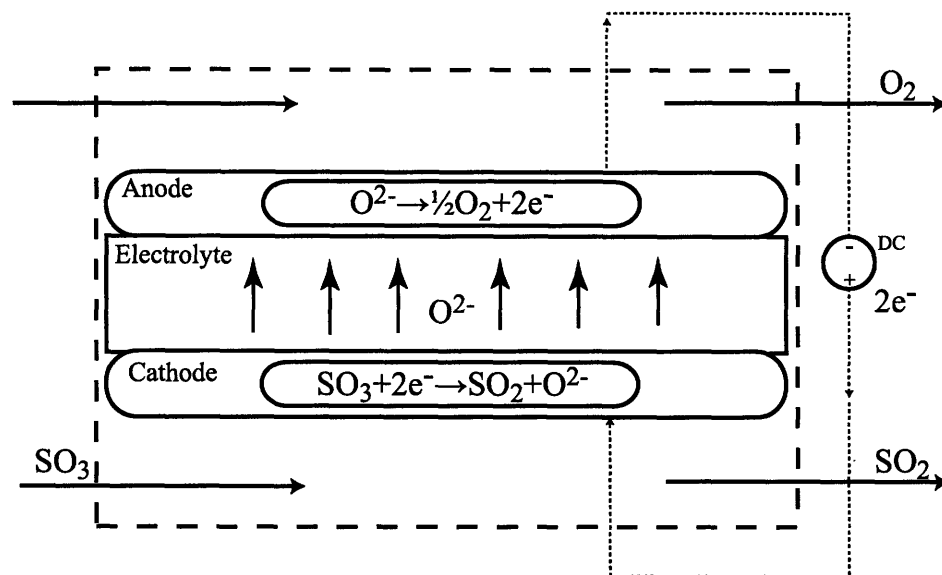
Figure 4-5: Conceptual design of sulfur dioxide decomposition electrolysis cell

4.3 System Optimization

The potential flow system for the sulfur hybrid cycle is much more complicated than previously described systems. A complete flow diagram is shown in Appendix B. The diagram is shown with strategically placed heat exchangers, compressors, and pumps. An extensive optimization for this single electrolyzer cycle was performed by Jeong et.al. [33].

4.3.1 Thermal Acid Decomposition

In this section, the contribution of operating conditions final percentage (in moles) of sulfur dioxide in the thermal acid decomposer will be presented. The work presented here was also used for the system modeling and optimization published by Jeong et. al. [33]. Modeling of the thermal acid decomposition in this cycle is also the subject of independent research [34].

Temperature
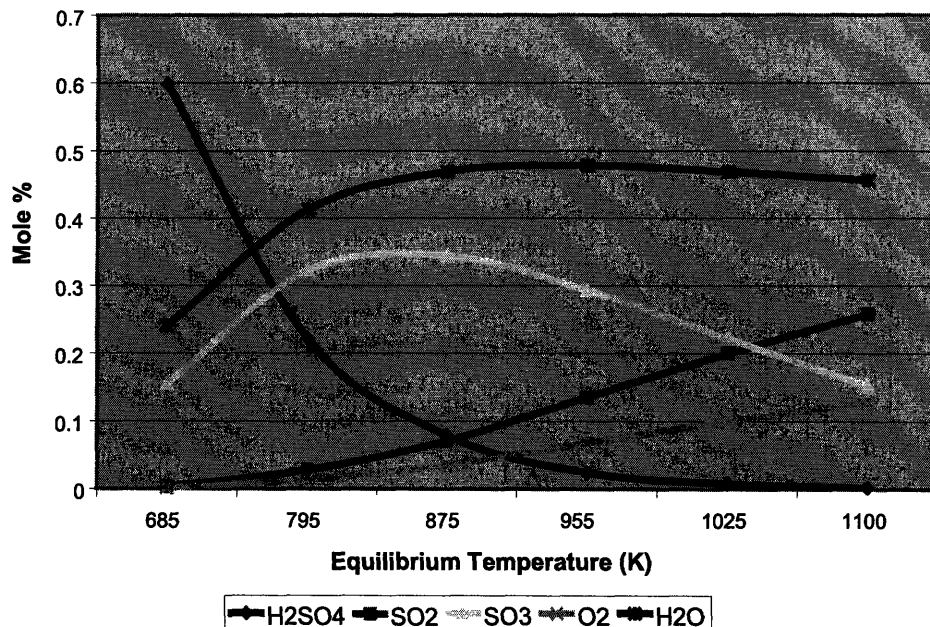
Figure 4-6: Mole fraction of chemical components in the decomposition reaction as a function of temperature, at 90% H_2SO_4 inlet concentration, with volume and pressure (7 bar) held constant

Temperature has a large effect on the decomposition completed at equilibrium. At higher temperatures, the acid decomposition (Reaction (4.2)) is driven closer to completion. This trend is illustrated in Figure 4-6. These calculations were performed using the widely used chemical thermodynamics software CHEMKIN [Reaction Design Inc., 2004]. The figure clearly shows the decomposition progression. The first chemical to decompose is the sulfuric acid, decomposing into sulfur trioxide and water. This reaction begins at a lower temperature with the fraction of sulfur trioxide increasing with increasing temperature until its own decomposition becomes dominant. At higher temperatures, sulfur partially decomposes into sulfur dioxide and oxygen.

Inlet Acid Concentration
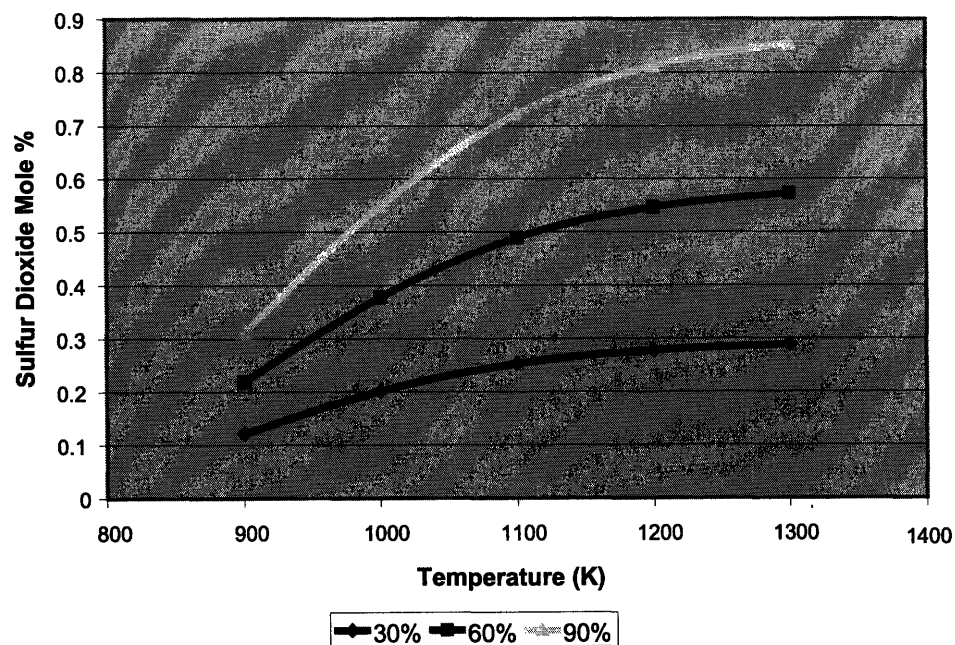
Figure 4-7: Mole fraction of sulfur dioxide in the decomposition reaction as a function of temperature and acid inlet concentration: assuming constant volume and pressure (1 bar)

Inlet acid concentration also plays a role in the total decomposition at equilibrium. At the inlet, aqueous sulfuric acid is fed into the decomposer. The effect of lower acid inlet concentrations on outlet mole fraction of sulfur dioxide is shown in Figure 4-7. The high inlet concentration of sulfuric acid leads to a higher outlet concentration of sulfur dioxide. Additionally, higher temperatures amplify the effect of the increased inlet concentration.

Pressure

Pressure is also important in the thermodynamics of decomposition. The equilibrium concentrations of all chemical components are calculated at a constant pressure, and Figure 4-8 illustrates the effect that this pressure has on the outlet fraction of sulfur
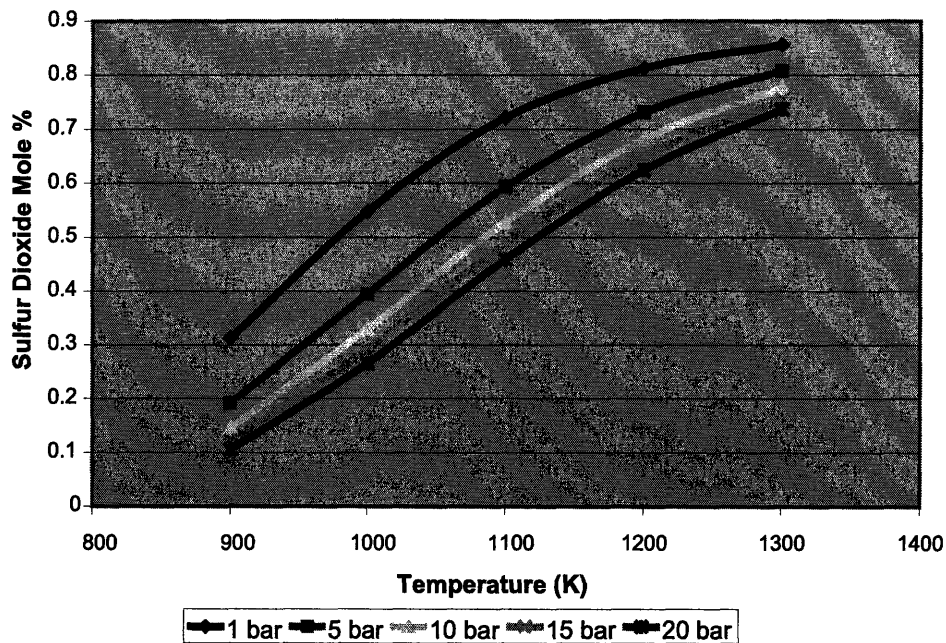
Figure 4-8: Mole fraction of sulfur dioxide in the decomposition reaction as a function of temperature and acid inlet concentration, assuming constant volume and pressure

dioxide. As shown, the completion of decomposition is greatest at low decomposer pressures. Overall, neglecting other system considerations, the highest thermal decomposition in the decomposer occurs when temperature and inlet concentration of sulfuric acid are high and the pressure is low.

Oxygen Concentration

The effect of incomplete decomposition upon the chemical components remaining in the cycle, and therefore returning to the inlet of the decomposer, is also important. Figure 4-9 illustrates the relationship between the inlet concentration of oxygen fed into the decomposer (1%) on the reaction completion at different inlet acid concentrations. Figure 4-9 also shows there is a very slight decrease in the decomposition completion inside the decomposer, but completion is virtually independent of acid inlet concentration with temperature.
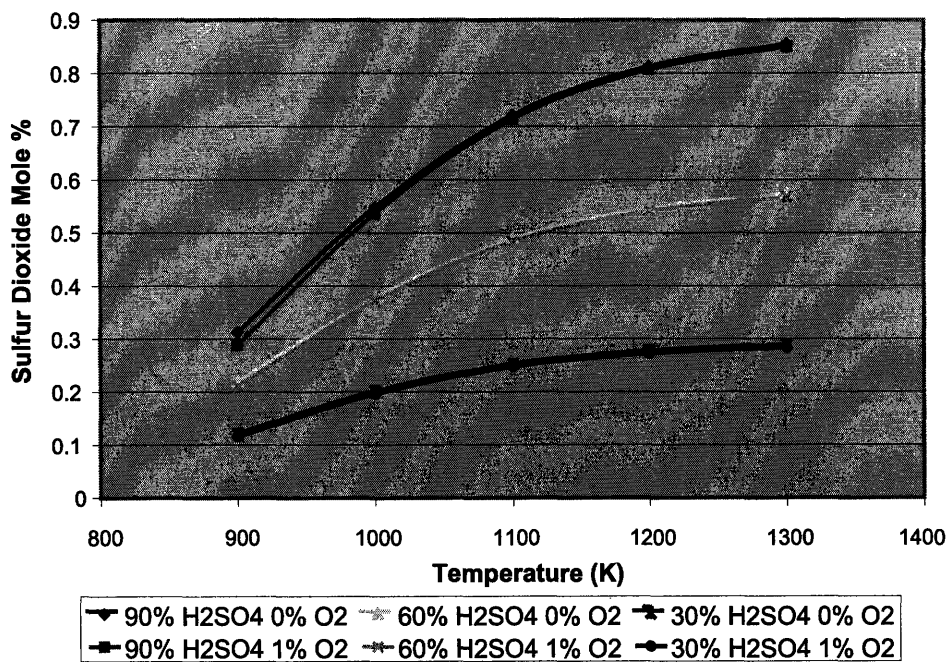
Figure 4-9: Mole fraction of sulfur dioxide in the decomposition reaction as a function of temperature, acid inlet concentration, and oxygen content, assuming constant volume and pressure (1 bar)

Figure 4-10 compares the decomposition completion with decomposer pressure. By varying decomposer pressure, a temperature dependant variation in decomposition due to oxygen content can be seen. At low decomposer temperatures and high decomposer pressure, the oxygen inlet concentration begins to decrease the decomposition completion. This sensitivity of decomposition to the additional chemical component at inlet reinforces the conclusion that the thermal decomposer should be operated at low pressures and high temperatures, thus avoiding this decrease in decomposition.
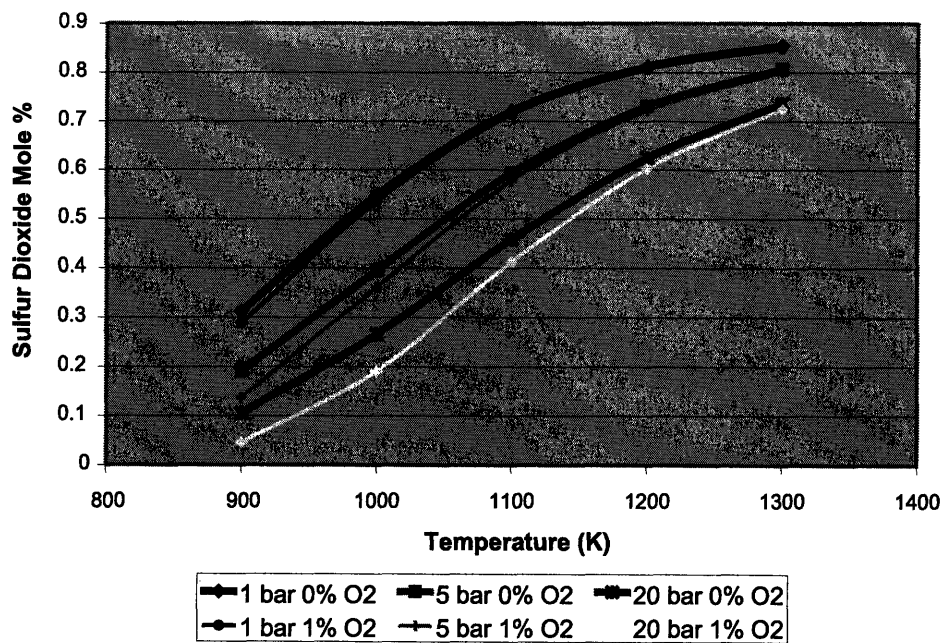
Figure 4-10: Mole fraction of sulfur dioxide in the decomposition reaction as a function of temperature, decomposer pressure, oxygen content, assuming constant volume and pressure

Chapter 5

Load Requirements

5.1 Introduction

In addition to being used in transportation, hydrogen also shows promise as an energy storage medium. Much of the electric production capacity in the United States is used only part of the time. This large production capacity is necessary to meet periods of high demand, but wasted at lower demand times since actual consumption can be far below capacity. Electricity demand fluctuates on daily, weekly, and seasonal timeframes. Daily, demand has a prolonged peak during normal business, with a secondary peak after sunset. Demand is then very low in the very early hours of the morning. An example of this trend can be seen in Figure 5-1(a).
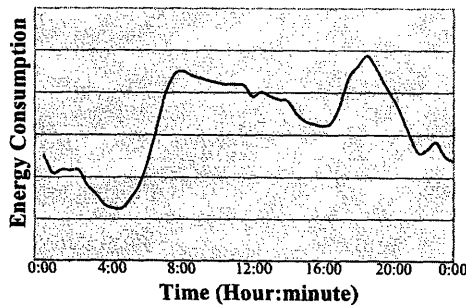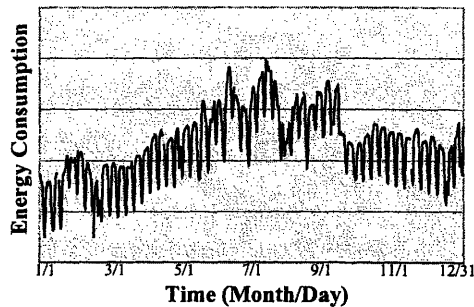
(a) Load Curve (Day)   (b) Load Curve (Year)

On a weekly basis, electricity demand drops off on the weekends, when many businesses are closed. Similarly, on an annual basis, demand is highly dependant upon the region. For example, in regions where cooling is necessary, the yearly peaks are in the summertime, during the hottest months. In northern climates more electricity is demanded for lighting during the shorter days of the winter. Finally, the region's heating source is important. In most regions, heating oil or natural gas is relied on heavily for heating needs. However, electricity may also be used for heating, in which case there will also be a peak during the coldest months. An example of both the weekly and annual trends can be seen in Figure 5-1(b).

While the magnitude of the electricity demand can be predicted in a general way, unexpected increases in customer demand (due to inclimate weather for example) or unexpected losses of generating supply (due to equipment outages for example) make it impossible to accurately predict the amount of electricity production needed at all times. The electricity grid is therefore run with a buffer of excess supply. This buffer is called the capacity margin, and in the United States is approximately 15% on average [35]. This means that on average, the electricity generating stations in the United States can produce 15% more electricity than is used on the grid. Maintaining capacity margins is important, because if the demand were to suddenly exceed the supply, the grid may experience blackouts.

While the average capacity margin is only 15%, the capacity margins during low demand times of the day can be substantially higher. If this offpeak capacity could be used to produce hydrogen, the power infrastructure could be used much more efficiently. In particular, large nuclear and coal plants are not easily manipulated to vary their output hourly or even daily. They are better off working at a base load all the time. This chapter seeks to expand on the previous reports on the feasibility of hydrogen production coupled with a nuclear power plant by looking at the feasibility of variable hydrogen production. With a variable production system, hydrogen could be produced during offpeak hours. During high demand times, the plant could return

then to supplying electricity to the grid. The previous work discussed in Chapter 3 has examined full capacity hydrogen production potential. However, in order to model this system, the effect of lowering hydrogen production from maximum to low capacity production was looked at.

5.2 Hydrogen / Electricity Production
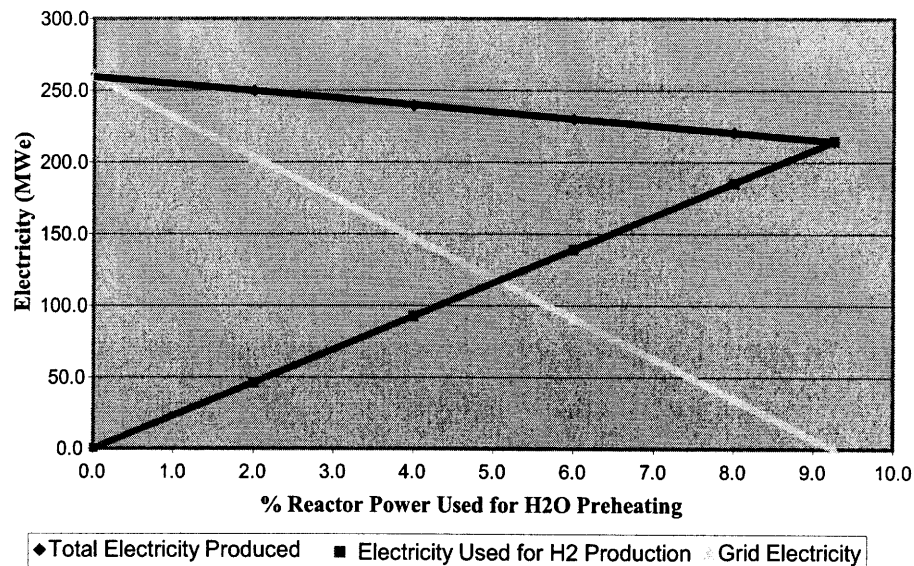
Figure 5-1: Electricity production broken into hydrogen process requirement and electricity distribution potential as a function of thermal energy extraction

Using the full energy potential of the reactor to produce hydrogen will leave no availability for the power producing potential of the power plant. For each of the configurations presented in Yildiz [32], approximately 9 to 10% of the reactor energy is diverted thermally to preheat the water for the hydrogen production system. By decreasing that thermal energy percentage, the production of hydrogen decreases, however energy is then available for excess electricity production that can be sold

to the grid. This can be accomplished by increasing the ratio of power system to
heat exchanger flow rates, discussed in 3.3.1 and illustrated in Figure 3-4(b). Figure
5-1 shows the tradeoff between the maximum hydrogen production and maximum
electricity production as a function of how much thermal energy is taken from the
reactor stream.

Figure 5-1 shows that the total electricity produced decreases as hydrogen pro-
duction increases. This relationship is caused by the fact that more and more thermal
energy is being diverted from the reactor, decreasing the thermal energy being sup-
plied to the turbine. This specific figure is for a reactor outlet of $550°C$ and system
pressure of 0.1MPa, and the same trend is shown through all temperatures and pres-
sures.

5.2.1 Cycle Efficiency
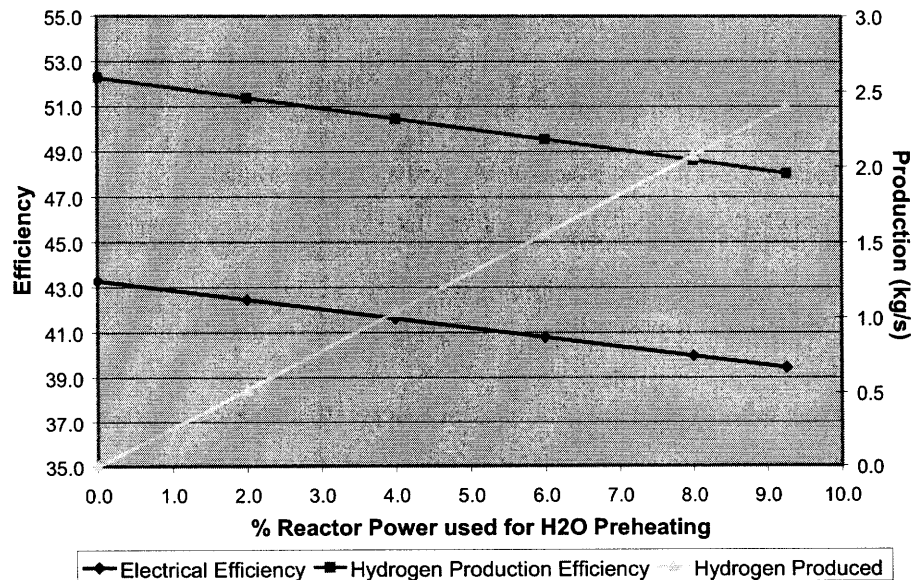
Figure 5-2: Electrical and process efficiencies and hydrogen production as a function
of thermal power extraction

A full description of the procedure for determining cycle efficiency is described in Section 3.3.2 and is also discussed in Yildiz [32]. Using these techniques, the process efficiency for a range of hydrogen production levels can be calculated, and is shown in Figure 5-2. This efficiency is calculated using the low heating value of hydrogen, and includes the initial pumping requirement for each system pressure. Figure 5-2 again shows the decreasing energy potential and efficiency as thermal energy is extracted from the reactor stream. The figure also shows the strong correlation between electrical efficiency and the hydrogen production efficiency. This correlation is strong because, unlike thermo-chemical cycles, the majority of the energy input into the high temperature electrolysis process for water splitting is in the form of electricity. Again, the relationships shown in the figure apply to all pressure and temperature ranges studied.

Chapter 6

Incomplete Decomposition

6.1 Introduction

When designing these cycles it is important to consider the speed at which the decomposition reactions can be conducted (the kinetics of the reaction). The kinetics determine how quickly reactants can be turned into products, and thus limits the production capability of the processes. In addition to the absolute speed of the reaction, it is also important to consider that complete reaction is only possible as with an infinite time of residence. In a realistic process, complete reaction will not be achieved, and the system must be designed to either tolerate or compensate for this. There are a few ways to improve the kinetics of reactions, and these improvements will be discussed in this Chapter, along with the effects that incomplete decomposition has upon both the HTSE and Hybrid Sulfur process designs.

6.2   Kinetics of Decomposition Reactions

6.2.1   Catalysts

Catalysts are widely used in industrial reactions. These catalysts serve to improve the kinetics of the reactions. The catalyst improves the reaction rate by providing an alternative reaction pathway with lower activation energy. Catalysts have been studied for the hybrid sulfur cycle primary electrolyzer [36][37], and for water electrolysis cells [24].

6.2.2   Thermal Decomposition

There are two important decomposition steps in the cycles examined. First the thermal decomposition of sulfuric acid into sulfur trioxide and water. This process is thermodynamically favored at temperatures above $350°C$, and is used in all variations of the hybrid sulfur cycle. This decomposition is governed by kinetic rates, defined by the Arhenius equation (Equation (6.1)).

$$k = Ae^{-\frac{E_{act}}{RT}} \qquad (6.1)$$

Where the rate k is dependant upon the activation energy, E_{act}, the temperature, T, and the frequency factor, A.

The second important thermal decomposition is the decomposition of sulfur trioxide into sulfur dioxide and oxygen in the thermal acid decomposition variation of the hybrid sulfur cycle. This reaction will also be governed by the Arhenius equation. Unfortunately, the exact reaction rates for these reactions have not been experimentally defined.

6.2.3 Electrochemical Decomposition

The rate of electrochemical decomposition is dependant upon the current being driven through the cell. This current is governed by what is called the ButlerVolmer Equation (Equation (6.2)).

$$i = i_o \left[e^{\frac{\alpha n F \eta_{act}}{RT}} - e^{\frac{(1-\alpha) n F \eta_{act}}{RT}} \right] \tag{6.2}$$

The current (i) is described in terms of the exchange current, i_o, and the activation overpotential, η_{act}, that are defined in Section 2.6. The production rate in the cell increases with the current. For example, in a water electrolysis cell, one molecule of hydrogen is produced for every electron that is driven through the system. Therefore the current flowing through the cell is directly proportional to the hydrogen production in the cell.

6.3 Varying Kinetic Rates and Plant Design

6.3.1 High Temperature Steam Electrolysis

Because HTSE is not a cycle, incomplete decomposition in the electrolysis cell will not substantially effect any of the components prior to the cell in the system. The only consequence of incomplete decomposition in the HTSE cell is additional steam leftover in the hydrogen out-stream. In order to compensate for the additional steam, a separator can be added along the exit stream, utilizing the cooling of the mixture to condense the steam to a liquid that can be diverted from the final product stream.

6.3.2 Hybrid Sulfur Cycle

Incomplete decomposition in the Hybrid Sulfur Cycle is a much more important concern as the cyclic nature of this process will cause all remaining chemicals to be cycled

back through the system. This means that the presence of sulfur dioxide, sulfur tri-oxide, and sulfuric acid must all be prepared for at all points in the system. Potential solutions to this problem are designing the system for tolerance of additional chemi-cals, or additional separation within the cycle. Additional separation is problematic because it necessarily cannot be complete either, and it also removes chemicals from what is designed to be a closed cycle.

Sulfur Dioxide

Excess sulfur dioxide may appear in the cycle if there is incomplete decomposition in the primary heat exchanger. This sulfur dioxide would be able to move through the system eventually to reenter the electrolyzer. Because of the general stability of the compound, the only adverse effect of its recirculation should be the slight decrease in efficiency due to the decrease in concentration of the active compounds in the decomposer.

Sulfuric Acid / Sulfur Trioxide

The effect of the excess sulfuric acid and sulfur trioxide in the system has a much bigger impact. Ideally, the sulfuric acid would be completely decomposed in the acid decomposer section of the hybrid sulfur process. This decomposition can be done thermally, with sulfuric acid decomposing into sulfur trioxide and water readily above temperatures at approximately $350°C$. However there are sections of the process where the temperatures drop below $350°C$, where sulfur trioxide would recombine in the aqueous solution to form sulfuric acid. If the non-decomposed sulfur trioxide is not completely removed from the flow stream after the acid decomposer, sulfuric acid will be circulated through the system. This will have an adverse effect in sensitive environments such as the primary electrolyzer where the corrosivity of the acid will undermine the material stability of the cell. In common cell materials such as zirconia oxide, the formation of sulfates at operating temperatures is thermodynamically fa-

vored in the presence of sulfuric acid and sulfur trioxide. The formation of sulfates on the electrolyte will slowly decrease the throughput of the cell until production ceases. In order to prevent this cell degradation, the tolerance of the electrolytic cells to the sulfur atmosphere must be verified experimentally, and controls must be implemented in the system to remain under tolerance levels.

Chapter 7

Conclusion

7.1   Non-Carbon Hydrogen Production Systems

United States hydrogen production today relies heavily on decomposition of natural gas or methane. There are many different cycles proposed that could produce hydrogen without relying on carbon sources. These cycles use combinations of thermal, electrical, and chemical energy to split water into hydrogen and oxygen. Two promising cycles that have been examined here are the high temperature steam electrolysis cycle and the hybrid sulfur cycle. Modeling has been done for assessment of the efficiency of both cycles.

For the high temperature steam electrolysis cycle, initial models have been created using heat recuperation techniques and a reactor heat source. The results from these models help illustrate the importance of certain design parameters such as system pressure, contrasting the system's potential production role with its potential efficiency.

The hybrid sulfur cycle has also been modeled and show a clear contrast between thermal and electrical variations of the cycle. The thermal acid decomposition variation uses direct heat as the energy source that allows the chemical energy to be recycled through the system. This has the benefit of using a direct heat source,

avoiding losses in energy due to the inefficiencies of energy conversion.

The second hybrid sulfur variation uses electrical energy to decompose and recycle the chemical components of the system. This variation is beneficial because it allows much lower process temperatures and high throughput.

7.2   Load Dependant Capabilities

In order to maximize the productive usage of power production facilities, excess energy in low grid demand periods can be converted to energy storage in the form of hydrogen. By allowing a reactor's power to be diverted back and forth from grid power to hydrogen production, the reactor becomes much more versatile and productive. These load dependant hydrogen production systems allow for variable storage of base energy.

7.3   Incomplete Decomposition Effects

In any realistic system, processes such as decomposition and separation will not be driven to completion. Thus the tolerances of the systems to excess chemical flows must be carefully considered when designing the final system. For high temperature steam electrolysis this is not a significant issue, as there are no chemicals that must be recycled back into the system. However with the hybrid sulfur cycle it is important that all of the sulfur compounds remain in the system. Not only that certain sulfur compounds present in certain parts of the cycle will be detrimental in any large quantities in other parts of the system. It is important to the system to compensate for incomplete decomposition to prevent material instability, lowered efficiency and production, and other adverse effects.

7.4 Future Work

The model used for coupling the high temperature steam electrolysis to a reactor needs to be expanded. A model developed with the coupling in mind will be much more flexible and accurate in predicting the production and efficiencies within the system. in addition, a new model built specifically for this purpose would allow for further exploration of more extensive questions, such as the feasibility of load dependant production.

The viability of the hybrid sulfur cycle is dependant on the discovery and development of materials that can be used effectively in the sulfur environment, specifically in the electrolysis cells. The sulfur environment presents unique challenges to material selection not present in water electrolysis cells. Not only cell stability, but also the efficiency of current densities throughout the cell must be optimized for this new environment.

Another topic of future study in the modeling capabilities for the hybrid sulfur cycle is the acquisition of kinetics data for most of the sulfur compound reactions of interest at the temperatures of interest. With more accurate kinetics data, more accurate models of the decomposition, especially the thermal decomposition, of these compounds can be created. This is important in order to understand the throughput that can realistically be achieved in a this system. Additionally, data must also be gathered for potential catalysts and the associated kinetics for these reactions.

Appendix A

Abbreviations and Symbols

A	frequency factor
D_{AB}	binary diffusivity of gas A into gas B (m^2/s)
E_{act}	activation energy (J/mol)
F	Faraday's constant : 96487 C/mol
Δ G	Gibbs free energy (J/mol)
Δ H	enthalpy (J/mol)
HTSE	High Temperature Steam Electrolysis
i	current (A)
i_l	limiting current density (A)
i_o	exchange current density (A)
k	rate constant (s^{-1})
M_x	molecular weight of x (kg/kmol)
n_e	number of electrons
P_x	partial pressure of x
R	universal gas constant: 8.314 J/mol K
Δ S	entropy (J/mol K)
SOEC	Solid Oxide Electrolysis Cell
T	temperature (K)

T_p	pyrolysis temperature
V_{min}	Nernst potential (V)
W_X	Work of X (W)

Greek Symbols

α	electrode transfer coefficient
δ	thickness (m)
γ	pre-exponential coefficient (A/m^2)
ϵ	porosity
η	overpotentials (V)
τ	tortuosity
σ	molecular diameter (m)
Ω	gas property

Appendix B

Hybrid Sulfur Optimization

Appendix C

HTSE Load Calculations

Reactor Exit Temperature, $T_{R,out}$ (°C): 550 — Electrolysis Pressure (MPa): 0.1 — Reversible Cell Voltage, E (V): -0.936 — Over-Potential (% of E): 0 — Reactor Power (MWth): 600

Power for H2O Preheating, F(%)	9.3	8.0	6.0	4.0	2.0	0.0
Power for H2O Preheating (MWth)	55.6	48.0	36.0	24.0	12.0	0.0
Reactor Inlet Temperature, $T_{R,in}$ (°C)	387.5	389.7	393.0	396.2	399.3	402.3
Reactor Inlet Enthalpy (kJ/kg)	835.3	838.0	842.1	846.0	849.8	853.4
Total Enthalpy Change (kJ/kg)	200.2	197.6	193.5	189.5	185.8	182.1
Ratio of flow rates, (m_{CO2}/m_{H2})	1247	1463	1993	3051	6226	-
Electrical Efficiency, η_{el} (%)	39.4	40.0	40.8	41.6	42.5	43.3
Process H2 Efficiency, η_{PH} (LHV, %)	48.0	48.6	49.5	50.5	51.4	52.3
Overall H2 Efficiency, η_{OH} (LHV, %)	42.4	42.9	43.6	44.3	45.0	45.7
kg H2 Produced (kg/s)	2.4	2.1	1.6	1.0	0.5	0.0
Electricity Produced (Mwe)	214.7	220.5	230.1	239.7	249.7	259.7
Electricity Used, H2 Production (Mwe)	214.6	185.4	139.1	92.7	46.4	0.0
Grid Energy Production (Mwe)	0.0	35.1	91.0	147.0	203.3	259.7

Reactor Exit Temperature, $T_{R,out}$ (°C): 650 — Electrolysis Pressure (MPa): 0.1 — Reversible Cell Voltage, E (V): -0.936 — Over-Potential (% of E): 0 — Reactor Power (MWth): 600

Power for H2O Preheating, F(%)	9.9	8.0	6.0	4.0	2.0	0.0
Power for H2O Preheating (MWth)	59.3	48.0	36.0	24.0	12.0	0.0
Reactor Inlet Temperature, $T_{R,in}$ (°C)	471.9	475.5	479.2	482.7	486.0	489.3
Reactor Inlet Enthalpy (kJ/kg)	938.7	943.2	947.7	952.0	956.2	960.2
Total Enthalpy Change (kJ/kg)	221.6	217.2	212.7	208.4	204.2	200.2
Ratio of flow rates, (m_{CO2}/m_{H2})	1055	1331	1813	2775	5663	-
Electrical Efficiency, η_{el} (%)	42.4	43.2	44.1	45.0	45.9	46.9
Process H2 Efficiency, η_{PH} (LHV, %)	51.3	52.2	53.2	54.2	55.1	56.1
Overall H2 Efficiency, η_{OH} (LHV, %)	45.0	45.7	46.4	47.2	47.9	48.6
kg H2 Produced (kg/s)	2.6	2.1	1.6	1.0	0.5	0.0
Electricity Produced (Mwe)	229.1	238.7	248.9	259.4	270.2	281.1
Electricity Used, H2 Production (Mwe)	229.2	185.4	139.1	92.7	46.4	0.0
Grid Energy Production (Mwe)	-0.1	53.2	109.9	166.7	223.8	281.1

Reactor Exit Temperature, $T_{R,out}$ (°C): 700 — Electrolysis Pressure (MPa): 0.1 — Reversible Cell Voltage, E (V): -0.936 — Over-Potential (% of E): 0 — Reactor Power (MWth): 600

Power for H2O Preheating, F(%)	10.2	8.0	6.0	4.0	2.0	0.0
Power for H2O Preheating (MWth)	60.9	48.0	36.0	24.0	12.0	0.0
Reactor Inlet Temperature, $T_{R,in}$ (°C)	514.5	518.8	522.6	526.3	529.8	533.2
Reactor Inlet Enthalpy (kJ/kg)	991.3	996.6	1001.3	1005.8	1010.1	1014.3
Total Enthalpy Change (kJ/kg)	232.2	226.9	222.2	217.7	213.3	209.2
Ratio of flow rates, (m_{CO2}/m_{H2})	981	1274	1735	2657	5421	-
Electrical Efficiency, η_{el} (%)	43.6	44.6	45.6	46.5	47.4	48.4
Process H2 Efficiency, η_{PH} (LHV, %)	52.6	53.7	54.7	55.7	56.7	57.7
Overall H2 Efficiency, η_{OH} (LHV, %)	46.0	46.8	47.6	48.3	49.1	49.8
kg H2 Produced (kg/s)	2.6	2.1	1.6	1.0	0.5	0.0
Electricity Produced (Mwe)	235.2	246.3	256.9	267.8	278.9	290.1
Electricity Used, H2 Production (Mwe)	235.3	185.4	139.1	92.7	46.4	0.0
Grid Energy Production (Mwe)	-0.1	60.9	117.9	175.1	232.5	290.1

Reactor Exit Temperature, $T_{R,out}$ (°C): 550 — Electrolysis Pressure (MPa): 0.1 — Reversible Cell Voltage, E (V): -0.936 — Over-Potential (% of E): 10 — Reactor Power (MWth): 600

Power for H2O Preheating, F(%)	8.6	8.0	6.0	4.0	2.0	0.0
Power for H2O Preheating (MWth)	51.3	48.0	36.0	24.0	12.0	0.0
Reactor Inlet Temperature, $T_{R,in}$ (°C)	388.7	389.7	393.0	396.2	399.3	402.3
Reactor Inlet Enthalpy (kJ/kg)	836.8	838.0	842.1	846.0	849.8	853.4
Total Enthalpy Change (kJ/kg)	198.7	197.6	193.5	189.5	185.8	182.1
Ratio of flow rates, (m_{CO2}/m_{H2})	1361	1463	1993	3051	6226	-
Electrical Efficiency, η_{el} (%)	39.7	40.0	40.8	41.6	42.5	43.3
Process H2 Efficiency, η_{PH} (LHV, %)	44.4	44.6	45.4	46.3	47.1	48.0
Overall H2 Efficiency, η_{OH} (LHV, %)	39.5	39.7	40.4	41.1	41.7	42.4
kg H2 Produced (kg/s)	2.2	2.1	1.6	1.0	0.5	0.0
Electricity Produced (Mwe)	218.0	220.5	230.1	239.7	249.7	259.7
Electricity Used, H2 Production (Mwe)	218.0	204.0	153.0	102.0	51.0	0.0
Grid Energy Production (Mwe)	0.0	16.5	77.1	137.7	198.7	259.7

Reactor Exit Temperature, $T_{R,out}$ (°C): 650 — Electrolysis Pressure (MPa): 0.1 — Reversible Cell Voltage, E (V): -0.936 — Over-Potential (% of E): 10 — Reactor Power (MWth): 600

Power for H2O Preheating, F(%)	9.1	8.0	6.0	4.0	2.0	0.0
Power for H2O Preheating (MWth)	54.8	48.0	36.0	24.0	12.0	0.0
Reactor Inlet Temperature, $T_{R,in}$ (°C)	473.3	475.5	479.2	482.7	486.0	489.3
Reactor Inlet Enthalpy (kJ/kg)	940.5	943.2	947.7	952.0	956.2	960.2
Total Enthalpy Change (kJ/kg)	219.8	217.2	212.7	208.4	204.2	200.2
Ratio of flow rates, (m_{CO2}/m_{H2})	1152	1331	1813	2775	5663	-
Electrical Efficiency, η_{el} (%)	42.7	43.2	44.1	45.0	45.9	46.9
Process H2 Efficiency, η_{PH} (LHV, %)	47.4	47.9	48.8	49.7	50.6	51.5
Overall H2 Efficiency, η_{OH} (LHV, %)	41.9	42.3	43.0	43.7	44.4	45.1
kg H2 Produced (kg/s)	2.4	2.1	1.6	1.0	0.5	0.0
Electricity Produced (Mwe)	232.9	238.7	248.9	259.4	270.2	281.1
Electricity Used, H2 Production (Mwe)	232.8	204.0	153.0	102.0	51.0	0.0
Grid Energy Production (Mwe)	0.1	34.7	96.0	157.5	219.2	281.1

Reactor Exit Temperature, $T_{R,out}$ (°C): 700 — Electrolysis Pressure (MPa): 0.1 — Reversible Cell Voltage, E (V): -0.936 — Over-Potential (% of E): 10 — Reactor Power (MWth): 600

Power for H2O Preheating, F(%)	9.4	8.0	6.0	4.0	2.0	0.0
Power for H2O Preheating (MWth)	56.3	48.0	36.0	24.0	12.0	0.0
Reactor Inlet Temperature, $T_{R,in}$ (°C)	516.1	518.8	522.6	526.3	529.8	533.2
Reactor Inlet Enthalpy (kJ/kg)	993.2	996.6	1001.3	1005.8	1010.1	1014.3
Total Enthalpy Change (kJ/kg)	230.3	226.9	222.2	217.7	213.3	209.2
Ratio of flow rates, (m_{CO2}/m_{H2})	1071	1274	1735	2657	5421	-
Electrical Efficiency, η_{el} (%)	44.0	44.6	45.6	46.5	47.4	48.4
Process H2 Efficiency, η_{PH} (LHV, %)	48.7	49.3	50.2	51.2	52.1	53.0
Overall H2 Efficiency, η_{OH} (LHV, %)	42.9	43.4	44.1	44.9	45.6	46.3
kg H2 Produced (kg/s)	2.4	2.1	1.6	1.0	0.5	0.0
Electricity Produced (Mwe)	239.1	246.3	256.9	267.8	278.9	290.1
Electricity Used, H2 Production (Mwe)	239.2	204.0	153.0	102.0	51.0	0.0
Grid Energy Production (Mwe)	0.0	42.3	104.0	165.8	227.9	290.1

Table 1 — Over-Potential = 0% of E

Parameter	550						650						700					
Reactor Exit Temperature, $T_{R,out}$ (°C)	550	550	550	550	550	550	650	650	650	650	650	650	700	700	700	700	700	700
Electrolysis Pressure (MPa)	1	1	1	1	1	1	1	1	1	1	1	1	1	1	1	1	1	1
Reversible Cell Voltage, E (V)	-0.994						-0.994						-0.994					
Over-Potential (% of E)	0						0						0					
Reactor Power (MWth)	600						600						600					
Power for H2O Preheating, F (%)	9.1	8.0	6.0	4.0	2.0	0.0	9.7	8.0	6.0	4.0	2.0	0.0	10.0	8.0	6.0	4.0	2.0	0.0
Power for H2O Preheating (MWth)	54.6	48.0	36.0	24.0	12.0	0.0	58.3	48.0	36.0	24.0	12.0	0.0	59.8	48.0	36.0	24.0	12.0	0.0
Reactor Inlet Temperature, $T_{R,in}$ (°C)	387.8	389.7	393.0	396.2	399.3	402.3	472.2	475.5	479.2	482.7	486.0	489.3	514.9	518.8	522.6	526.3	529.8	533.2
Reactor Inlet Enthalpy (kJ/kg)	835.6	838.0	842.1	846.0	849.8	853.4	939.2	943.2	947.7	952.0	956.2	960.2	991.8	996.6	1001.3	1005.8	1010.1	1014.3
Total Enthalpy Change (kJ/kg)	199.9	197.6	193.5	189.5	185.8	182.1	221.2	217.2	212.7	208.4	204.2	200.2	231.7	226.9	222.2	217.7	213.3	209.2
Ratio of flow rates, (m_{CO_2}/m_{H_2})	1322	1522	2072	3172	6473	-	1120	1384	1885	2886	5889	-	1041	1325	1804	2762	5637	-
Electrical Efficiency, η_{el} (%)	39.5	40.0	40.8	41.6	42.5	43.3	42.5	43.2	44.1	45.0	45.9	46.9	43.7	44.6	45.6	46.5	47.4	48.4
Process H2 Efficiency, η_{PH_2} (LHV, %)	45.4	45.9	46.7	47.6	48.5	49.3	48.5	49.3	50.2	51.1	52.0	52.9	49.7	50.7	51.6	52.6	53.5	54.5
Overall H2 Efficiency, η_{OH} (LHV, %)	44.1	44.6	45.4	46.2	47.0	47.9	47.1	47.8	48.7	49.5	50.4	51.3	48.3	49.1	50.0	50.9	51.8	52.7
kg H2 Produced (kg/s)	2.3	2.0	1.5	1.0	0.5	0.0	2.4	2.0	1.5	1.0	0.5	0.0	2.5	2.0	1.5	1.0	0.5	0.0
Electricity Produced (Mwe)	215.4	220.5	230.1	239.7	249.7	259.7	230.0	238.7	248.9	259.4	270.2	281.1	236.1	246.3	256.9	267.8	278.9	290.1
Electricity Used, H2 Production (Mwe)	215.5	189.5	142.1	94.7	47.4	0.0	230.0	189.5	142.1	94.7	47.4	0.0	236.1	189.5	142.1	94.7	47.4	0.0
Grid Energy Production (Mwe)	-0.1	31.0	87.9	145.0	202.3	259.7	0.0	49.2	106.8	164.7	222.8	281.1	-0.1	56.8	114.8	173.0	231.5	290.1

Table 2 — Over-Potential = 10% of E

Parameter	550						650						700					
Reactor Exit Temperature, $T_{R,out}$ (°C)	550	550	550	550	550	550	650	650	650	650	650	650	700	700	700	700	700	700
Electrolysis Pressure (MPa)	1	1	1	1	1	1	1	1	1	1	1	1	1	1	1	1	1	1
Reversible Cell Voltage, E (V)	-0.994						-0.994						-0.994					
Over-Potential (% of E)	10						10						10					
Reactor Power (MWth)	600						600						600					
Power for H2O Preheating, F (%)	8.4	8.0	6.0	4.0	2.0	0.0	9.0	8.0	6.0	4.0	2.0	0.0	9.2	8.0	6.0	4.0	2.0	0.0
Power for H2O Preheating (MWth)	50.3	48.0	36.0	24.0	12.0	0.0	53.8	48.0	36.0	24.0	12.0	0.0	55.3	48.0	36.0	24.0	12.0	0.0
Reactor Inlet Temperature, $T_{R,in}$ (°C)	389.0	389.7	393.0	396.2	399.3	402.3	473.7	475.5	479.2	482.7	486.0	489.3	516.4	518.8	522.6	526.3	529.8	533.2
Reactor Inlet Enthalpy (kJ/kg)	837.2	838.0	842.1	846.0	849.8	853.4	552.4	943.2	947.7	952.0	956.2	960.2	993.6	996.6	1001.3	1005.8	1010.1	1014.3
Total Enthalpy Change (kJ/kg)	198.4	197.6	193.5	189.5	185.8	182.1	607.9	217.2	212.7	208.4	204.2	200.2	229.8	226.9	222.2	217.7	213.3	209.2
Ratio of flow rates, (m_{CO_2}/m_{H_2})	1445	1522	2072	3172	6473	-	441	1384	1885	2886	5889	-	1136	1325	1804	2762	5637	-
Electrical Efficiency, η_{el} (%)	39.8	40.0	40.8	41.6	42.5	43.3	42.8	43.2	44.1	45.0	45.9	46.9	44.1	44.6	45.6	46.5	47.4	48.4
Process H2 Efficiency, η_{PH_2} (LHV, %)	41.9	42.0	42.8	43.6	44.4	45.2	44.8	45.2	46.0	46.9	47.7	48.6	46.0	46.5	47.4	48.3	49.1	50.0
Overall H2 Efficiency, η_{OH} (LHV, %)	40.8	41.0	41.7	42.5	43.3	44.0	43.6	44.0	44.8	45.6	46.4	47.2	44.7	45.2	46.0	46.9	47.7	48.5
kg H2 Produced (kg/s)	2.1	2.0	1.5	1.0	0.5	0.0	2.2	2.0	1.5	1.0	0.5	0.0	2.3	2.0	1.5	1.0	0.5	0.0
Electricity Produced (Mwe)	218.7	220.5	230.1	239.7	249.7	259.7	233.7	238.7	248.9	259.4	270.2	281.1	240.0	246.3	256.9	267.8	278.9	290.1
Electricity Used, H2 Production (Mwe)	218.6	208.4	156.3	104.2	52.1	0.0	233.7	208.4	156.3	104.2	52.1	0.0	240.0	208.4	156.3	104.2	52.1	0.0
Grid Energy Production (Mwe)	0.1	12.1	73.7	135.5	197.6	259.7	0.0	30.2	92.6	155.2	218.1	281.1	0.1	37.9	100.6	163.6	226.7	290.1

Table (Electrolysis Pressure = 2 MPa, Reversible Cell Voltage E_r = -1.012 V, Over-Potential = 0% of E_r, Reactor Power = 600 MWth)

Reactor Exit Temperature, $T_{R,out}$ (°C)	550						650						700					
Power for H2O Preheating, F (%)	9.0	8.0	6.0	4.0	2.0	0.0	9.6	8.0	6.0	4.0	2.0	0.0	9.9	8.0	6.0	4.0	2.0	0.0
Power for H2O Preheating (MWth)	54.1	48.0	36.0	24.0	12.0	0.0	57.8	48.0	36.0	24.0	12.0	0.0	59.3	48.0	36.0	24.0	12.0	0.0
Reactor Inlet Temperature, $T_{R,in}$ (°C)	387.9	389.7	393.0	396.2	399.3	402.3	472.4	475.5	479.2	482.7	486.0	489.3	515.1	518.8	522.6	526.3	529.8	533.2
Reactor Inlet Enthalpy (kJ/kg)	835.8	838.0	842.1	846.0	849.8	853.4	939.4	943.2	947.7	952.0	956.2	960.2	992.0	996.6	1001.3	1005.8	1010.1	1014.3
Total Enthalpy Change (kJ/kg)	199.7	197.6	193.5	189.5	185.8	182.1	221.0	217.2	212.7	208.4	204.2	200.2	231.5	226.9	222.2	217.7	213.3	209.2
Ratio of flow rates, (m_{CO2}/m_{H2})	1346	1534	2088	3197	6525	-	1139	1395	1900	2908	5935	-	1059	1335	1818	2784	5681	-
Electrical Efficiency, η_{el} (%)	39.5	40.0	40.8	41.6	42.5	43.3	42.5	43.2	44.1	45.0	45.9	46.9	43.7	44.6	45.6	46.5	47.4	48.4
Process H2 Efficiency, η_{H2} (LHV, %)	44.7	45.1	46.0	46.8	47.7	48.5	47.7	48.4	49.4	50.3	51.2	52.1	49.0	49.8	50.8	51.7	52.6	53.6
Overall H2 Efficiency, η_{oH2} (LHV, %)	44.3	44.7	45.5	46.4	47.2	48.0	47.2	48.0	48.9	49.7	50.6	51.5	48.5	49.3	50.2	51.2	52.1	53.0
kg H2 Producted (kg/s)	2.2	2.0	1.5	1.0	0.5	0.0	2.4	2.0	1.5	1.0	0.5	0.0	2.4	2.0	1.5	1.0	0.5	0.0
Electricity Produced (Mwe)	215.8	220.5	230.1	239.7	249.7	259.7	230.4	238.7	248.9	259.4	270.2	281.1	236.5	246.3	256.9	267.8	278.9	290.1
Electricity Used, H2 Production (Mwe)	215.7	191.3	143.5	95.7	47.8	0.0	230.3	191.3	143.5	95.7	47.8	0.0	236.6	191.3	143.5	95.7	47.8	0.0
Grid Energy Production (Mwe)	0.0	29.2	86.5	144.1	201.8	259.7	0.1	47.3	105.4	163.8	222.3	281.1	-0.1	55.0	113.4	172.1	231.0	290.1

Table (Electrolysis Pressure = 2 MPa, Reversible Cell Voltage E_r = -1.012 V, Over-Potential = 10% of E_r, Reactor Power = 600 MWth)

Reactor Exit Temperature, $T_{R,out}$ (°C)	550						650						700					
Power for H2O Preheating, F (%)	8.3	8.0	6.0	4.0	2.0	0.0	8.9	8.0	6.0	4.0	2.0	0.0	9.1	8.0	6.0	4.0	2.0	0.0
Power for H2O Preheating (MWth)	49.9	48.0	36.0	24.0	12.0	0.0	53.4	48.0	36.0	24.0	12.0	0.0	54.8	48.0	36.0	24.0	12.0	0.0
Reactor Inlet Temperature, $T_{R,in}$ (°C)	389.1	389.7	393.0	396.2	399.3	402.3	473.8	475.5	479.2	482.7	486.0	489.3	516.6	518.8	522.6	526.3	529.8	533.2
Reactor Inlet Enthalpy (kJ/kg)	837.3	838.0	842.1	846.0	849.8	853.4	941.1	943.2	947.7	952.0	956.2	960.2	993.8	996.6	1001.3	1005.8	1010.1	1014.3
Total Enthalpy Change (kJ/kg)	198.2	197.6	193.5	189.5	185.8	182.1	219.3	217.2	212.7	208.4	204.2	200.2	229.7	226.9	222.2	217.7	213.3	209.2
Ratio of flow rates, (m_{CO2}/m_{H2})	1470	1534	2088	3197	6525	-	1242	1395	1900	2908	5935	-	1155	1335	1818	2784	5681	-
Electrical Efficiency, η_{el} (%)	39.8	40.0	40.8	41.6	42.5	43.3	42.8	43.2	44.1	45.0	45.9	46.9	44.1	44.6	45.6	46.5	47.4	48.4
Process H2 Efficiency, η_{H2} (LHV, %)	41.2	41.3	42.1	42.9	43.7	44.5	44.0	44.4	45.3	46.1	47.0	47.8	45.2	45.7	46.6	47.5	48.3	49.2
Overall H2 Efficiency, η_{oH2} (LHV, %)	40.9	41.0	41.8	42.5	43.3	44.1	43.7	44.0	44.9	45.7	46.5	47.3	44.8	45.3	46.2	47.0	47.8	48.7
kg H2 Producted (kg/s)	2.1	2.0	1.5	1.0	0.5	0.0	2.2	2.0	1.5	1.0	0.5	0.0	2.3	2.0	1.5	1.0	0.5	0.0
Electricity Produced (Mwe)	219.0	220.5	230.1	239.7	249.7	259.7	234.1	238.7	248.9	259.4	270.2	281.1	240.4	246.3	256.9	267.8	278.9	290.1
Electricity Used, H2 Production (Mwe)	218.9	210.5	157.9	105.2	52.6	0.0	234.2	210.5	157.9	105.2	52.6	0.0	240.5	210.5	157.9	105.2	52.6	0.0
Grid Energy Production (Mwe)	0.1	10.0	72.2	134.5	197.0	259.7	-0.1	28.2	91.1	154.2	217.6	281.1	-0.1	35.8	99.1	162.5	226.2	290.1

Table (Over-Potential = 0)

Reactor Exit Temperature, $T_{R,out}$ (°C)	550						650						700					
Electrolysis Pressure (MPa)	3						3						3					
Reversible Cell Voltage, E, (V)	-1.022						-1.022						-1.022					
Over-Potential (% of E)	0						0						0					
Reactor Power (MWth)	600						600						600					
Power for H2O Preheating, F (%)	9.0	8.0	6.0	4.0	2.0	0.0	9.6	8.0	6.0	4.0	2.0	0.0	9.8	8.0	6.0	4.0	2.0	0.0
Power for H2O Preheating (MWth)	53.7	48.0	36.0	24.0	12.0	0.0	57.4	48.0	36.0	24.0	12.0	0.0	58.9	48.0	36.0	24.0	12.0	0.0
Reactor Inlet Temperature, $T_{R,in}$ (°C)	388.0	389.7	393.0	396.2	399.3	402.3	472.5	475.5	479.2	482.7	486.0	489.3	515.2	518.8	522.6	526.3	529.8	533.2
Reactor Inlet Enthalpy (kJ/kg)	836.0	838.0	842.1	846.0	849.8	853.4	939.5	943.2	947.7	952.0	956.2	960.2	992.1	996.6	1001.3	1005.8	1010.1	1014.3
Total Enthalpy Change (kJ/kg)	199.6	197.6	193.5	189.5	185.8	182.1	220.8	217.2	212.7	208.4	204.2	200.2	231.3	226.9	222.2	217.7	213.3	209.2
Ratio of flow rates, (m_{CO2}/m_{H2})	1359	1535	2091	3201	6532	-	1149	1397	1902	2912	5942	-	1069	1337	1820	2787	5688	-
Electrical Efficiency, η_{el} (%)	39.6	40.0	40.8	41.6	42.5	43.3	42.5	43.2	44.1	45.0	45.9	46.9	43.8	44.6	45.6	46.5	47.4	48.4
Process H2 Efficiency, η_{PH} (LHV, %)	44.3	44.7	45.5	46.4	47.2	48.0	47.3	48.0	48.9	49.8	50.7	51.6	48.5	49.4	50.3	51.2	52.1	53.1
Overall H2 Efficiency, η_{OH} (LHV, %)	44.3	44.7	45.5	46.4	47.2	48.0	47.3	48.0	48.9	49.8	50.7	51.6	48.5	49.4	50.3	51.2	52.1	53.1
kg H2 Produced (kg/s)	2.2	2.0	1.5	1.0	0.5	0.0	2.4	2.0	1.5	1.0	0.5	0.0	2.4	2.0	1.5	1.0	0.5	0.0
Electricity Produced (Mwe)	216.1	220.5	230.1	239.7	249.7	259.7	230.8	238.7	248.9	259.4	270.2	281.1	236.9	246.3	256.9	267.8	278.9	290.1
Electricity Used, H2 Production (Mwe)	216.0	193.1	144.8	96.5	48.3	0.0	230.7	193.1	144.8	96.5	48.3	0.0	236.9	193.1	144.8	96.5	48.3	0.0
Grid Energy Production (Mwe)	0.1	27.4	85.2	143.2	201.4	259.7	0.0	45.6	104.1	162.9	221.9	281.1	0.0	53.2	112.1	171.2	230.6	290.1

Table (Over-Potential = 10)

Reactor Exit Temperature, $T_{R,out}$ (°C)	550						650						700					
Electrolysis Pressure (MPa)	3						3						3					
Reversible Cell Voltage, E, (V)	-1.022						-1.022						-1.022					
Over-Potential (% of E)	10						10						10					
Reactor Power (MWth)	600						600						600					
Power for H2O Preheating, F (%)	8.3	8.0	6.0	4.0	2.0	0.0	8.8	8.0	6.0	4.0	2.0	0.0	9.1	8.0	6.0	4.0	2.0	0.0
Power for H2O Preheating (MWth)	49.6	48.0	36.0	24.0	12.0	0.0	53.0	48.0	36.0	24.0	12.0	0.0	54.4	48.0	36.0	24.0	12.0	0.0
Reactor Inlet Temperature, $T_{R,in}$ (°C)	389.2	389.7	393.0	396.2	399.3	402.3	473.9	475.5	479.2	482.7	486.0	489.3	516.7	518.8	522.6	526.3	529.8	533.2
Reactor Inlet Enthalpy (kJ/kg)	837.4	838.0	842.1	846.0	849.8	853.4	941.3	943.2	947.7	952.0	956.2	960.2	994.0	996.6	1001.3	1005.8	1010.1	1014.3
Total Enthalpy Change (kJ/kg)	198.1	197.6	193.5	189.5	185.8	182.1	219.1	217.2	212.7	208.4	204.2	200.2	229.5	226.9	222.2	217.7	213.3	209.2
Ratio of flow rates, (m_{CO2}/m_{H2})	1483	1535	2091	3201	6532	-	1254	1397	1902	2912	5942	-	1166	1337	1820	2787	5688	-
Electrical Efficiency, η_{el} (%)	39.8	40.0	40.8	41.6	42.5	43.3	42.9	43.2	44.1	45.0	45.9	46.9	44.1	44.6	45.6	46.5	47.4	48.4
Process H2 Efficiency, η_{PH} (LHV, %)	40.8	40.9	41.7	42.5	43.3	44.1	43.7	44.0	44.8	45.7	46.5	47.3	44.8	45.3	46.2	47.0	47.9	48.7
Overall H2 Efficiency, η_{OH} (LHV, %)	40.8	40.9	41.7	42.5	43.3	44.1	43.7	44.0	44.8	45.7	46.5	47.3	44.8	45.3	46.2	47.0	47.9	48.7
kg H2 Produced (kg/s)	2.0	2.0	1.5	1.0	0.5	0.0	2.2	2.0	1.5	1.0	0.5	0.0	2.2	2.0	1.5	1.0	0.5	0.0
Electricity Produced (Mwe)	219.3	220.5	230.1	239.7	249.7	259.7	234.4	238.7	248.9	259.4	270.2	281.1	240.7	246.3	256.9	267.8	278.9	290.1
Electricity Used, H2 Production (Mwe)	219.3	212.4	159.3	106.2	53.1	0.0	234.4	212.4	159.3	106.2	53.1	0.0	240.8	212.4	159.3	106.2	53.1	0.0
Grid Energy Production (Mwe)	0.0	8.1	70.8	133.5	196.6	259.7	0.0	26.3	89.7	153.3	217.1	281.1	-0.1	33.9	97.7	161.6	225.8	290.1

Bibliography

[1] (2006, Mar.) Hydrogen facts and figures. U.S. Department of Energy. [Online]. Available: http://www.hydrogen.energy.gov/facts_figures.html

[2] G. A. Olah, A. Goeppert, and G. K. S. Prakash, *Beyond Oil and Gas: The Methanol Economy.* Weinham: WILEY-VCH Verlag GmbH & Co. KGaA, 2006.

[3] D. Pile, D. Doughty, and J. O. Keller, "Increasing the efficiency of the water electrolysis cell," in *DOE Hydrogen Program 2005 Annual Progress Report*, 2005, ch. IV.H.6, pp. 353–356.

[4] S. Porter, "Hydrogen generation from electrolysis," in *DOE Hydrogen Program 2005 Annual Progress Report*, 2005, ch. IV.H.7, pp. 357–360.

[5] R. Perret, Y. Chen, G. Besenbruch, R. Diver, A. Weimer, A. Lewandowski, and E. Miller, "Solar hydrogen generation research," in *DOE Hydrogen Program 2005 Annual Progress Report*, 2005, ch. IV.I.1, pp. 377–388.

[6] P. S. Pickard, F. Gelbard, J. Andazola, and G. Naranjo, "Sulfur-iodine thermochemical cycle," in *DOE Hydrogen Program 2005 Annual Progress Report*, 2005, ch. IV.G.2, pp. 296–300.

[7] M. B. Gorensek, W. A. Summers, M. R. Buckner, and Z. H. Qureshi, "Conceptual design and projected performance for a hybrid sulfur process," in

American Institute of Chemical Engineers (AIChE'05), Cincinnati, Ohio, Oct. 30 – Nov. 4, 2005, paper 348c.

[8] R. D. Doctor, D. C. Wade, and M. H. Mendelsohn, "STAR-H2: A calcium-bromine hydrogen cycle using nuclear heat," in *American Institute of Chemical Engineers (AIChE'02)*, New Orleans, LA, Mar. 10–14, 2002, paper 139c.

[9] J. S. Herring, J. E. O'Brien, C. M. Stoots, P. Lessing, W. Windes, D. Wendt, M. G. McKellar, M. Sohal, and G. L. Hawkes, "High-temperature electrolysis," in *DOE Hydrogen Program 2005 Annual Progress Report*, 2005, ch. IV.G.1, pp. 291–295.

[10] J. A. Ruud, "System design and new materials for reversible solid-oxide high-temperature steam electrolysis," in *DOE Hydrogen Program 2005 Annual Progress Report*, 2005, ch. IV.H.8, pp. 361–362.

[11] I. I. Balachov, S. Crouch-Baker, M. Hornbostel, M. McKubre, A. Sanjurjo, and F. Tanzella, "Modular system for hydrogen generation and oxygen recovery," in *DOE Hydrogen Program 2005 Annual Progress Report*, 2005, ch. IV.H.9, pp. 363–366.

[12] C. M. Stoots, J. E. O'Brien, M. G. McKellar, G. L. Hawkes, and J. S. Herring, "Engineering process model for high-temperature steam electrolysis system performance evaluation," in *American Institute of Chemical Engineers (AIChE'05)*, Cincinnati, Ohio, Oct. 30 – Nov. 4, 2005, paper 348a.

[13] C. Stoots, J. E. O'Brien, J. S. Herring, and P. A. Lessing, "Hydrogen production from nuclear energy via high temperature electrolysis," in *International Congress on Advances in Nuclear Power Plants (ICAPP'04)*, Pittsburgh, PA, 13–17 2004.

[14] W. A. Summers and M. R. Buckner, "Hybrid sulfur thermochemical process development," in *DOE Hydrogen Program 2005 Annual Progress Report*, 2005, ch. IV.G.7, pp. 323–328.

[15] J. W. Weidner, "Low temperature electrolytic hydrogen production," in *DOE Hydrogen Program 2005 Annual Progress Report*, 2005, ch. IV.I.3, pp. 392–395.

[16] J. P. O'Connell, K. P. Bellezza, P. Narkpresert, M. B. Gorensek, and P. M. Mathias, "Thermodynamic efficiency analysis of the S-I process for nuclear hydrogen production," in *American Institute of Chemical Engineers (AIChE'05)*, Cincinnati, Ohio, Oct. 30 – Nov. 4, 2005, paper 258a.

[17] B. L. Bischoff, D. F. Wilson, L. E. Powell, and K. D. Adcock, "Applicability of inorganic membranes for the production of hydrogen using nuclear energy," in *American Institute of Chemical Engineers (AIChE'05)*, Cincinnati, Ohio, Oct. 30 – Nov. 4, 2005, paper 258e.

[18] B. L. Bischoff, L. D. Trowbridge, L. K. Mansur, and C. W. Forsberg, "Production of hydrogen using nuclear energy and inorganic membranes," in *International Congress on Advances in Nuclear Power Plants (ICAPP'04)*, Pittsburgh, PA, 13–17 2004.

[19] M. A. Lewis, "High-temperature thermochemical processes," in *DOE Hydrogen Program 2005 Annual Progress Report*, 2005, ch. IV.G.3, pp. 301–305.

[20] D. F. Wilson, "Materials for high-temperature thermochemical processes," in *DOE Hydrogen Program 2005 Annual Progress Report*, 2005, ch. IV.G.6, pp. 319–322.

[21] M. A. Wilson and C. Lewinsohn, "Characterization of candidate ceramic materials for the high temperature sulfuric acid loop in the si process," in *American Institute of Chemical Engineers (AIChE'05)*, Cincinnati, Ohio, Oct. 30 – Nov. 4, 2005, paper 405b.

[22] S. Suyama, T. Kameda, Y. Itoh, and N. Handa, "Development of high strength reaction sintered silicon carbide for hydrogen production system," in *International Congress on Advances in Nuclear Power Plants (ICAPP'04)*, Pittsburgh, PA, 13–17 2004.

[23] B. Chi, H. Lin, J. Li, N. Wang, and J. Yang, "Comparison of three preparation methods of $NiCo_2O_4$ electrodes," *International Journal of Hydrogen Energy*, vol. 31, pp. 1210–1214, 2006.

[24] N. Osada, H. Uchida, and M. Watanabe, "Polarization behavior of sdc cathode with highly dispersed ni catalysts for solid oxide electrolysis cells," *Journal of The Electrochemical Society*, vol. 153, no. 5.

[25] J. R. Mawdsley, D. J. Myers, and B. Yildiz, "Materials development for improved efficiency of hydrogen production by steam electrolysis and thermochemical-electrochcemcial processes," in *American Institute of Chemical Engineers (AIChE'05)*, Cincinnati, Ohio, Oct. 30 – Nov. 4, 2005, paper 348b.

[26] S. R. Sherman, "Progress in high temperature materials and systems in the U.S. DOE nuclear hydrogen initiative," in *American Institute of Chemical Engineers (AIChE'05)*, Cincinnati, Ohio, Oct. 30 – Nov. 4, 2005, paper 405a.

[27] H. Görgün, "Dynamic modelling of a proton exchange membrane (PEM) electrolyzer," *International Journal of Hydrogen Energy*, vol. 31, pp. 29–38, 2006.

[28] S. A. Grigoriev, V. I. Porembsky, and V. N. Fateev, "Pure hydrogen production by PEM electrolysis for hydrogen energy," *International Journal of Hydrogen Energy*, vol. 31, pp. 171–175, 2006.

[29] A. Co, S. J. Xia, and V. I. Birss, "A kinetic study of the oxygen reduction reaction at $LaSrMnO_3 - YSZ$ composite electrodes," *Journal of the Electrochemical Society*, vol. 152, pp. A570–A576, 2005.

[30] C. J. Geankoplis, *Mass Transport Phenomena*. New York: Holt, Rinehart and Winston, Inc., 1972.

[31] V. Dostal, "A supercritical carbon dioxide cycle for next generation nuclear reactors," Ph.D. dissertation, Massachusetts Institute of Technology, Cambridge, MA, 2004.

[32] B. Yildiz, K. Hohnholt, and M. S. Kazimi, "Hydrogen production using high temperature steam electrolysis and gas reactors with supercritical CO_2 cycles," CANES, MA, Tech. Rep. MIT-NES-TR-002, Dec. 2004.

[33] Y. H. Jeong, M. S. Kazimi, K. J. Hohnholt, and B. Yildiz, "Optimization of the hybrid sulfur cycle for hydrogen generation," CANES, MA, Tech. Rep. MIT-NES-TR-004, May 2005.

[34] V. I. Ponyavin, "Application of conjugate heat transfer and flow analyses for design optimization of the SI decomposer," in *American Institute of Chemical Engineers (AIChE'05)*, Cincinnati, Ohio, Oct. 30 – Nov. 4, 2005, paper 405c.

[35] Energy Information Administration. (2004, Oct.) Electricity supply and demand fact sheet. [Online]. Available: http: //www.eia.doe.gov/cneaf/electricity/page/fact_sheets/supply&demand.html

[36] D. M. Ginosar, L. M. Petkovic, and K. C. Burch, "Activity and stability of sulfuric acid decomposition catalysts for thermochemical water splitting cycles," in *American Institute of Chemical Engineers (AIChE'05)*, Cincinnati, Ohio, Oct. 30 – Nov. 4, 2005, paper 258d.

[37] V. Barbarossa, S. Brutti, M. Diamanti, S. Sau, and G. De Maria, "Catalytic thermal decomposition of sulphuric acid in sulphur-iodine cycle for hydrogen production," *International Journal of Hydrogen Energy*, vol. 31, pp. 883–890, 2006.